Humidity measurements in moist gas conditions

Wolf, A.J.

Award date:
2011

Humidity measurements in moist gas conditions

Bram Wolf

TU/e - Physics/MTP department

accompanied by: Raoul Liew, Jos Zeegers
a.j.wolf@student.tue.nl

September 2011

Abstract

For characterisation of an experimental setup involving a vortex tube, the feasibility of determining the water content that is contained in a moist nitrogen gas flow has been explored. The fast flow rates and high moisture levels that can be expected result in challenging measurement conditions.

Based a closed-chamber and a continuous flow measurement approach, two measurement setups have been designed and built to measure the water content in moist nitrogen flows, using artificially generated sample mixtures. In both cases, heating is used to ensure the mixture is in a fully gaseous state before measurement occurs.

Using the closed-chamber method, experiments have been conducted to asses the measurement capabilities of the setup. The results indicate that the closed chamber measurement method is suitable for further fine-tuning and implementation in the vortex setup. The second measurement method has not been implemented due to time constraints. Taking into account the extra complexity of this setup, it is expected that acquiring accurate measurement result will be more challenging than with the closed-chamber method.

Contents

Chapter 1

Introduction

Ranque and Hilsh discovered the remarkable energy seperation processes in a vortex tube independently of one another in respectively 1933 and 1947. The so-called Ranque-Hilsh vortex tube is a device without moving parts which separates presurized gas in a cold and warm streams.

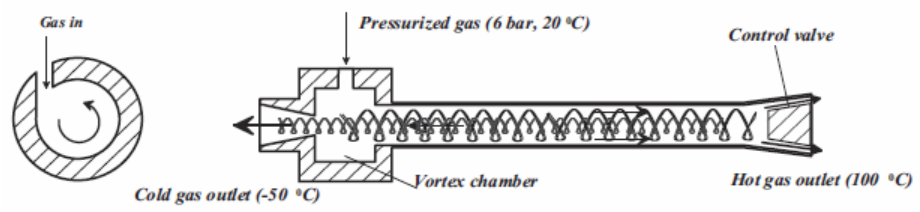

Figure 1.1: Vortex tube schematic

A cross-section of a typical vortex tube is displayed in Figure 1.1. The device works by injecting compressed gas into a vortex chamber where it is tangentially expanded and azimuthally accelerated. This process creates a vortex motion inside the vortex tube section of the apparatus. Due to complex flow mechanisms which are not yet fully understood[1], the gas breaks up into a relatively cool stream in the center of the tube and a hotter stream in the peripheral region of the tube. Outlets in the radial center and the perimeter of the tube at either ends give hot and cold exit streams.

The cooling properties of the vortex tube can be used to separate gas components from a homogeneous gas mixture input. Condensible components in a gas mixture may be separated by the cooling process inside the vortex tube, requiring only pressurized inflow of gas and no moving parts. Particularly interesting applications are found in gas extraction in situations where the quality of the gas suffers from carbon dioxide or water vapour dilution. A large number of gas fields is currently not economically viable due to the fact that large extraction costs are involved with the conventional separation techniques.

In the experimental test setup, a small scale vortex tube is used to research the feasibility of gas separation on industrial scale. In the setup, nitrogen gas at a pressure of

[1] Up to this date no agreement on a single explanation for the energy separation effect inside the vortex tube is found.

up to 10 bars is injected into the vortex tube, carrying water vapour and liquid droplets with a 1-50 μm diameter range. The droplets are used for 3D LDA measurements to map the gas flow speeds and directions at any point inside the vortex tube. The water content in the nitrogen is also used as condensible component to study the possibilities for separation of the gas mixture components.

For adequate evaluation of the separation process of water and nitrogen inside the vortex tube, the water content of the exit streams must be analysed. A method to measure the absolute amount of water carried by the hot and cold outlets has to be developed. The operating conditions of the vortex tube allow for the possibility of moist gas (containing both water vapour and liquid droplets) outflow and flow speeds up to 200 m3n/h and up to 20 g/m3 water content. Temperatures of the hot and cold outlet stream can range from -20$^\circ C$ to 100$^\circ C$.

This report is part of an 15 ECTS internship, which is part of the TU/e physics Bachelor programme. The first part of the internship involves a literature study in relevant subjects to all key aspects of the assignment. Secondly, designs for both measurement methods must be made based on the given design parameters. The last step will be to test the devices and verify if the desired measurements can be performed in the final setup.

Chapter 2

Mission Statement

The objective of this project is to determine the water content in a mixture of nitrogen gas, water vapour and liquid water droplets. The presence of liquid water within the gas makes it impossible to measure humidity levels with conventional humidity sensors alone. Considering the most simple solutions, two methods can be thought of to determine the total amount of water per volume (absolute humidity) of the flow:

- By heating, the saturation point of the gas is raised until all water is evaporated to the gaseous state. This eventually results in relative humidity levels which fall within the sub-saturated measuring window of typical humidity sensors.
- By cooling, the saturation point of the gas is lowered until (almost) all water is condensed. By measuring the volume or mass of the liquid water that is collected, the absolute humidity of the gas can be determined.

Both methods are used in industry, mostly on large scales. For the sake of simplicity and effectiveness the heating method is chosen. The small scale that is used for the experimental setup entails very small quantities of liquid water in the cooling method which can't be easily measured with high accuracy. The final measurement device, based on a prototype to be designed and tested during the internship, will be incorporated in the currently existing experimental setup.

Two measurement methods using the heating approach have been determined in advance. Both methods have the potential to work in the final setup and involve different challenges.

1. A *closed-chamber* measurement method incorporated in the exit flow of the vortex tube, delivering discrete measurement points. In a batch process, measurements can be taken in a captured 'flow segment' after it is heated to a certain point where all liquid water is evaporated. During measurement, the measurement chamber is closed to ensure conservation of the trapped mixture.
2. A *continuous* measurement method that constantly measures the water content levels of a passing gas flow. For this method to work, the entire flow that passes the measuring section must be preheated to evaporate all liquid water content. To avoid the unnecessary large heating requirements required to evaporate all liquid water in the entire vortex exit flow, a small portion is extracted, from the main flow using a sampling technique.

Chapter 3

Humidity and measurement techniques

The process to successfully determine the water content in a moist gas requires a thorough comprehension of all aspects that are involved with humidity. In this chapter the concepts of humidity, humidity sensors and humidity measurements are covered. Also the most convenient unit to express the water content in a sample is introduced.

Atmospheric humidity is a term that indicates the amount of water vapour that is carried by a gaseous volume. In most cases the atmospheric humidity refers to the water content in air, as this is an important characteristic in meteorology for instance, and has direct influence on various materials. It is also easily sensible by human beings because the thermal comfort that is experienced with the humidity level of the environment. Atmospheric humidity is commonly referred to as plainly *humidity*, as also from now on in this report. Humidity can be expressed in various ways, each being more or less sensitive to changes in various environmental factors like temperature and pressure. In the the following section the basic theory behind the concept of humidity will be treated. In the further sections the more advanced concepts and measurement devices and methods of measurement will be introduced.

3.1 Humidity Theory

Humidity refers to the water vapour content present in a gas. This doesn't mean that humid air is necessarily moist. A certain amount of water can be contained in a gas state by the air, without the formation of liquid droplets. Following the most common metric, humidity indicates the water content it contains relative to the maximal water content that can possibly be held at a specific temperature. This is therefore called the *relative humidity*, and is expressed as a percentage. Formally the relative humidity *RH* is defined as the ratio of the partial pressure $p_{(H_2O)}$ of the water vapour and the saturated vapor pressure $p^*_{(H_2O)}$.

$$RH = \frac{p_{(H_2O)}}{p^*_{(H_2O)}} \cdot 100\% \tag{3.1}$$

A	B	C	$T_{min}(^\circ C)$	$T_{max}(^\circ C)$
8,10765	1750,286	235,0	0	60
7,96681	1668,21	228,0	60	150

Table 3.1: Constants A, B and C associated with the vapour pressure of water.

3.1.1 Vapour pressure

The vapour pressure is the pressure that would be needed to achieve equilibrium between the in this case gaseous and liquid phases of the water in a closed system situation. The partial vapour pressure ranges between zero and the saturation vapour pressure. As soon as the saturation vapour pressure is exceeded, condensation of water occurs. So, following this line, the relative humidity can not exceed 100%.

Based on Antoine's equation 3.2,a approximation of the vapour pressure can be obtained in equation .

$$log_{10}p^*(T) = A - \frac{B}{C+T} \tag{3.2}$$

Depending on the compound, a specific set of constants A, B and C and temperature T in $^\circ C$ are required to calculate the corresponding saturation pressure. The constants and thus the vapour pressure are expressed in mmHg. The experimentally obtained constants for water accompanied with accuracy temperature range is displayed in table 3.1.1. [1]

To convert the vapour pressure from mmHg to pascals the equation is multiplied with a conversion factor of 133.322[8]. Also, the temperature T is converted from Celsius- to the Kelvin scale. This results in the following equations for the saturation vapour pressure in pascals:

$$\begin{aligned} p^*_{(H_2O)}(T) &= 133.322 \cdot 10^{8,10765-\frac{1750,286}{T-38.15}}, \quad 273 < T < 333 \\ p^*_{(H_2O)}(T) &= 133.322 \cdot 10^{7,96681-\frac{1668,21}{T-45.15}}, \quad 333 < T < 423 \end{aligned} \tag{3.3}$$

Here T is in Kelvin. Within the indicated accuracy range an average deviation of 0.2-0.9% from the actual value can be expected [2]. Using equation 3.1 the partial vapour pressure can be found with any given relative humidity and temperature.

$$p_{(H_2O)} = RH \cdot p^*_{(H_2O)}(T) \tag{3.4}$$

3.1.2 Absolute humidity

The term *absolute humidity* is used to define the amount of water vapour content in a given volume of carrier gas. More precisely, the absolute humidity on a volume basis is the mass of gaseous water m_w contained in the moist gas volume V_{net}. This differs from the dry-volume of the gas V_{dry} with the fact that the water in gaseous state V_w adds to the total volume. Therefore absolute humidity is only applicable to sub-saturated gasses in the strictest sense and can not be used to indicate the total amount of water in liquid and gaseous form in that is contained in the volume. The unit for the absolute humidity AH is grams per cubic meter.

$$AH = \frac{m_w}{V_{net}} = \frac{m_w}{V_{dry} + V_w}$$

Because the absolute humidity depends on the gas volume, a change in pressure or temperature will influence the absolute humidity. This is inconvenient for use in system calculations and analysis because temperatures and pressures are often not fixed. This problem is avoided by using the gas mass in stead of the volume.

3.1.3 Specific humidity and mass ratio

The fraction of water vapour mass over the total mass of water vapour plus carrier gas forms the *specific humidity*: SH. The specific humidity gives the mass percentage of water vapour contained in a gas mixture. In a closed system the specific humidity does not depend on changes in temperature or pressure as long as no evaporation occurs in order for the water vapour content to remain on a constant level.

$$SH = \frac{m_w}{m_g + m_w} \tag{3.5}$$

The ratio of vapour mass and *dry* carrier gas mass gives the *mixing ratio r*. In comparison to the specific humidity, the mixing ratio expresses the mass of water vapour with respect to the dry gas mass. This is an easier way to handle humidity when the dry gas mass is known, for instance when using a setup with a mass-flow meter that only measure the amount of dry carrier gas. An expression for the mixing ratio is given in equation 3.6[7]. Here ε is the molar mass ratio between the vapour material and the carrier gas. For water vapour in nitrogen, ε has a value of 0.622[8].

$$r = \frac{m_w}{m_g} = \frac{\varepsilon \cdot p_{(H_2O)}}{p - p_{(H_2O)}} \tag{3.6}$$

The absolute difference between the specific humidity and mixing ratio is small because the water vapour mass is typically small in comparison to the total volume. As can be derived from 3.5 and 3.1.2 the two units are simply connected with the expression

$$SH = \frac{r}{1 + r} \tag{3.7}$$

3.2 Sensor Performance and Measurement Quality

Generally, as long as a humidity sensor is used within it's specified zone of operation, the quality of the acquired measurements will meet the specifications provided by the manufacturer. When requiring measurements from specific samples of gas, the matter becomes more complicated. Details involving the different kinds of digital humidity sensors can be found in Appendix A

The most important attributes of humidity sensors can be summarized with the specifications listed below[9]. Most of these characteristics are specified by the manufacturers of recent high-end humidity sensors.

- *Accuracy*, often specified for certain relative humidity ranges
- Working *range*, ambient conditions (temperature/humidity) where accuracy is guaranteed.

- *Repeatablility*, measurement deviations due to *hysteresis* effects
- Long-term stability, also known as *drift*
- *Response time* to changes in humidity
- *Stabilization time*, also known as *start-up time*
- The ability to recover from condensation, also referred to as the *recovery time*
- Resistance to chemical compounds and debris
- Size
- Data acquisition and signal conditioning requirements

3.2.1 Sources of measurement error

Correct measurement of in samples is less straight-forward and introduces new factors that influence the measurement outcome. The following universal list of potential sources of error have been identified by the WMO[1] in measurement of humidity with humidity sensors[7].

- Modification of the air sample,for example by heat or water-vapor source or sink
- Contamination of the sensor
- Calibration error, including pressure correction
- Inappropriate treatment of water/ice phase
- Poor instrument design, for example temperature measurement error as result of heat conduction to sensor
- Incorrect operation, for example failure to achieve a stable equilibrium in the sample gas before measurement.
- Inappropriate sampling and/or averaging intervals

In a measurement setup involving humidity sensing, all these factors must be assessed and eliminated before reliable measurements can be taken. The amount of factors involved can make in a challenge to identify the source of error.

3.2.2 Sensor Response Time

The time constant of a humidity sensor is a specification that indicates the response of the sensor to a change in humidity. Generally a 64,2% (1/e) change in humidity is used to indicate the response time. Typical values for the most important humidity sensor types for scientific research are given in table 3.2.2. Time-constants are defined for measurements in still/quiescent surrounding conditions. When introducing a sensor head in a gas flow, reaction times can be even shorter than specified by the manufacturer.

[1] World Meteorologist Organisation

	1/e time-constant (s)		
Sensor Type	-20°*C*	0°*C*	20°*C*
Electrical capacitance	1-10	1-10	1-10
Electrical resistance	1-10	—	—
Thermal conductivity		16-50[2]	

Table 3.2: Constants *A*, *B* and *C* associated with the vapour pressure of water. capacitive 20-60 s time constant according to [9]

3.2.3 Sensor Filters

Protective filters are often used to shield humidity sensors from debris and containments (salt in maritime environment) introduced by the environment as these can negatively influence sensor performance. Most contaminations can be removed by various cleaning processes. Typical filter design covers the entire sensor and has a pore size that is adjusted to under the minimal size of the expected unwanted particles. However, the use of protective filters also negatively influences the response time of the filter by disabling a bulk movement of air past the sensor. The sensing process may have to partially or entirely rely on molecular diffusion for transportation through the filter rather that free air-flow, which may result in major time-constant increases. For controlled scientific measurements where it is possible to eliminate the flow of contaminants, a filter-less sensor setup is generally preferred over the protected equivalent.

Chapter 4

Heating theory

The heating requirements of the measurement setups involve several forms of heat transfer. In this chapter a summery of basic heat theory is given that will be used during the setup design. The numerical model used to estimate the required heating tube length for the continuous measurement setup is described in Appendix C. Based on these calculations, the dimensioning of the of the continuous method sampling system components are chosen.

4.1 Conductive heat transfer

Conduction of heat occurs without any visible or measurable form of movement. The heat flows through the material itself without requiring bulk motion of the matter. Solids, liquids and gasses all permit conductive heat transfer, of which the ease is characterized by the *thermal conductivity k*. Matter with a high thermal conductivity will conduct better than materials with low thermal conductivity. Mathematically conduction is described by Fourier's law which is displayed in equation 4.1.

$$\overrightarrow{q} = -k\nabla T \tag{4.1}$$

In this case $\overrightarrow{q}$ is the local heat flux density in W/m^2, k is the materials thermal conductivity in $W \cdot m^{-1} \cdot K^{-1}$ and ∇T is the temperature gradient expressed in K/m. The heat flux from a certain volume of material is expressed as a temperature change multiplied by the heat capacity of the material. Fouriers law becomes:

$$\rho c_p \frac{\partial T}{\partial t} = \phi - k\nabla^2 T \tag{4.2}$$

where ρ is the density while c_p is the heat capacity in $[J/m^3K]$. ϕ is a factor that is used to add heating sources within the volume in [J/s]. With no heating source, ϕ is zero. Combined with some rearrangements equation 4.2 turns into:

$$\frac{\partial T}{\partial t} = \kappa\nabla^2 T \tag{4.3}$$

the basic transient heat equation. κ is called the thermal diffusivity coefficient and arises from the aggregation of the three units. $\kappa = \frac{k}{\rho c_p}$.

With this partial differential equation transient heating profile problems within a heated cylinder can be calculated. Boundary values can be addressed to both the cylinder wall and the end 'caps' at two z-values. The solution will be a temperature profile $T(t,r,z)$ dependant on time, radial and axial coordinates. In the case of a long tube, the effects of the boundary caps of the cylinder can be neglected in the middle section of the tube. In this case the z term can be omitted. In cylinder coordinates (r,θ,z) with axial symmetry it changes to:

$$\frac{\partial T}{\partial t} = \kappa \left[\frac{1}{r} \frac{\partial}{\partial r} \left(r \frac{\partial T}{\partial r} \right) \right] \tag{4.4}$$

The steady state equivalent of equation 4.3 has no partial derivatives to the time as the problem has no time dependant conditions.

4.2 Convective heat transfer

Convection is the heat transfer mechanism that accounts for the transfer of energy between an object and its environment by fluid motion. Convection is usually dominant over conduction in liquids and gasses because temperature differences induce motion and therefore convective heat transfer [10]. A distinction must be made between *free- or natural convection* and *forced convection*. Free convection is caused by density differences that occur as a result of a temperature difference. Forced convection relies on imposed flow by external means. A further treatment of free convection is not needed.

Forced convection heat transfer (Newtons cooling law) 4.5 is a solution to the Fourier's law (equation 4.1).

$$\frac{dQ}{dt} = \overrightarrow{q} = h \cdot A \cdot \Delta T(t) \tag{4.5}$$

In equation 4.5, h is the *convective heat transfer coefficient* (assumed independent of t), A is the surface area of energy transfer and ΔT is the time-dependant difference between the object's heated surface area and the temperature of the environment suitably far from the surface so it is not influenced by the convection process. Newton's cooling law requires the conduction mechanism to be large compared to the convection mechanism to ensure a constant body temperature. In reality, the heat transfer coefficient changes with the temperature.

4.3 Radiative heat transfer

Radiated heat is transferred by means of energetic (mostly electromagnetic) particle emission. This mode starts playing a larger role at high temperatures and is therefore not further covered.

4.4 Biot number

The *Biot number* is a dimensionless number which characterises the resistance to heat transfer within the volume of a solid. It represents the ratio of convective over conductive heat transfer. The Biot number is defined as[11]:

$$Bi = \frac{hL_c}{k_b} \tag{4.6}$$

In this equation h is the heat transfer coefficient (or convective heat transfer coefficient), the characteristic length L_c is the ratio of volume over surface area in [m] and k_b is the bulk thermal conductivity of the volume [w/mK]. The heat transfer coefficient can be aquired when $\overrightarrow{q}$, A and ΔT are known by rewriting 4.5. In this case ΔT is defined as the temperature difference between the edge and the average temperature cross-section in the case the volume is encased in a pipe.

$Bi < 0,1$: Heat transfer mechanisms within the volume are high compared to the supply of heat at the edges of the volume. Temperature gradients within the volume are small and the bulk is taken as one unit of thermal mass.

$Bi > 1$: The temperature differences between edge and center of the volume are not to be neglected. Large temperature gradients is formed in this case.

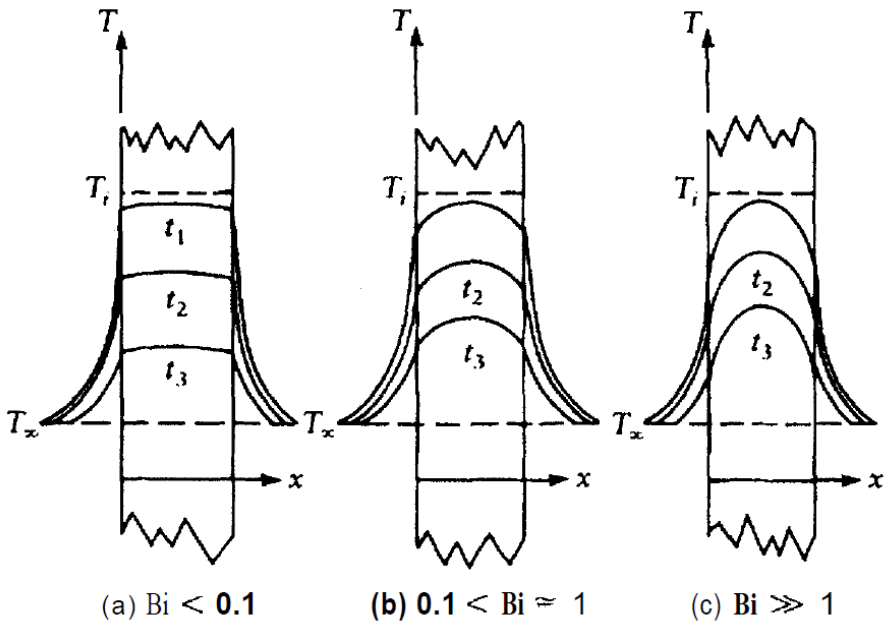

Figure 4.1: Temperature gradients of cylindrical volumes at extreme values (a) and (c), and an intermediate situation (b). T_i is the initial temperature profile and the development at three later moments in time t_1, t_2 and t_3 are shown for the three situations. (taken from Janna 2000 [11], pg192)

Chapter 5

Sampling and Transport of moist gas mixtures

Measuring the water content of the gas flows that exit the vortex tube requires some means of transportation to the measurement device. Transportation of moist gas samples without altering the mixture is complex . Due to various mechanisms, water droplets van easily be depositioned and thus lost due to evaporation and other mechanisms. Adding to the complexity, extracting part of the main gas flow may be necessary by means of sampling to improve measurably, in particular when dealing with large flowing rates. The concepts of sampling and transport of gas mixtures conveying particles in general will be covered in this chapter.

5.1 General Sampling Method

Aerosol measurement is used in a wide range of fields for a multitude of purposes. Frequently this involves the withdrawal of a sample of gas from a certain space of interest and the transportation to a measurement device. A sample inlet is used to extract the aerosol sample from the ambient environment. Special care must be given to the design, placement and orientation of the sample inlet, depending on the desired sampling performance for the each specific situation. Finally the samples will be withdrawn from either the hot or the cold outlet of the vortex tube.

5.2 Sampling Theory

Sampling theory is generally focused on solid aerosol particles, using absolute particle count as measure. The efficiency of the sampling process is defined as the ratio of particles leaving the sampling system over the amount of sampled particles. This is also called the sample efficiency η_{sample}. In the case of water-droplet aerosols, as will be the case in for this project, the aerosol count is actually not important. The absolute water content in both liquid and gaseous state is the value of interest. It is more meaningful to use the water content as a measure for efficiency in stead of the number of aerosols as this amount may vary due to evaporation, condensation. Losing droplets to mechanisms other than evaporation will result in unreliable measuring results, thus

requiring a total sampling efficiency that approaches 100% as close as possible.

$$\eta_{sample} = \frac{AH_{delivered}}{AH_{sampled}} \tag{5.1}$$

With this definition, aerosol loss due to droplet evaporation is effectively omitted as loss factor.

Reaching an optimal sampling efficiency requires good comprehension of all factors that inhibit the sampling process. A list of potential factors that can (negatively) influence sample efficiency associated with the sampling of moist gas is listed below.

1. Aspiration efficiency and deposition in the sampling inlet due to undesirable flow effects during sample extraction
2. Deposition during transport due to gravitational and inertial forces
3. Inhomogeneity in the ambient aerosol concentration
4. Agglomeration of particles during transport
5. Evaporation and condensation of aerosol material during transport
6. Re-entrainment of deposition material in the sample flow
7. High local deposition causing flow restriction of plugging

The above listed factors can be divided in two categories, namely inlet efficiency factors and transport efficiency factors. It is notable that apart from the first and third point in the above listed factors, all are associated with the *transportation* of the sample to the measuring device. The transport section of a sampling system often gets underestimated because all the action seems to happen at the inlet. However, due to the large amount of factors influencing the transportation efficiency, a efficient transportation system design is of crucial importance for good results.

Following the previously mentioned divide in the sampling system, formed by both an inlet and transportation, each with it's own considerations, leads to a alternative expression of equation 5.1 based on the separate efficiencies of both sections:

$$\eta_{sample} = \eta_{inlet}\eta_{transport} \tag{5.2}$$

The following sections will cover the efficiency components of equation 5.2.

5.2.1 Sample Extraction and Inlet Design

In the sampling process, the first step is to obtain a sample by extracting it from the environment. Given the application in this project, only the case in which the sampling takes place in a flowing medium will be covered. In this case the flow will be referred to as the *source*- or *main flow*.

Of the different nozzle designs, the *thin-walled sampling nozzle* is ideal for sampling in a continuous steady state flow. As opposed to alternative designs like thick-walled nozzles or blunt samplers, the thin-walled nozzle leads to little disturbance of the flow of gas and rebound of particles from the leading edge into the inlet is reduced to practically zero. The most simple thin-walled nozzle design is a round tube with thin walls that is suspended in the gas flow. Nozzles can be classified as thin-walled if

the ratio of internal and external diameter is less than 1.1[3], according to are made of a round tube with. Only thin-walled tube inlets will be treated in this section as this is clearly the way to go for the application.

The process of withdrawing aerosols from the environment into the sampling system is lead by the aspiration of aerosols and the transmission of them. The total inlet efficiency can therefore be expressed as a product of inlet aspiration efficiency and transmission efficiency.

$$\eta_{inlet} = \eta_{aspiration}\eta_{transmission} \tag{5.3}$$

The aspiration of aerosols involves the adoption of an ambient flow to the flow of the sampling nozzle, and it's efficiency is defined as the concentration of particles of particular size divided by their concentration in the surroundings. The transmission indicates the amount of particles of a specific size making it through the inlet to the transportation. The transmission efficiency is defined as the concentration of particles of particular size that are transmitted over the concentration of aspirated particles. Therefore the inlet efficiency in equation 5.3 is a function of particle size/mass.

The ambient gas stream velocity in the vicinity of the sampling inlet is U_0 and the sampling velocity, taken as the average gas flow velocity in the inlet is U. The efficiency of extracting a sample relies on both gravitational and inertial factors. Firstly the sampling velocity must be high enough to prevent gravitational setteling of the particles. Secondly the sampling velocity must be low enough to let the aerosol particles accommodate to the sampling flow. For this last condition, following basic inertia theory, small particles will more easily follow the flow. Larger particles with more mass will have more tendency to keep moving in the same direction.

The orientation of the nozzle with respect to both the gravitational field as the flow direction as also the absolute position have influence on the sampling behaviour. By convention, a nozzle is said to face upward if the sampling flow direction is downward. A nozzle facing the ambient flow is thus aligned with the flow and this is called *isoaxial sampling*. One speaks of an-isoaxial or non-isoaxial sampling when the ambient and sample flow directions are not parallel. The sampling speeds with respect to ambient flow rates can be chategorized in three situations. Sampling is said to be *iso-kinetic* when the sampling speed matches the ambient flow speed ($U = U_0$). The terms sub-isokinetic sampling and super-isokinetic sampling are used when the sampling velocity lower or higher than the ambient flow velocity ($U \neq U_0$). By convention this terminology applies to both laminar and turbulent ambient stream regimes.

Figure 5.1 shows a schematic representation of isoaxial sampling with a thin-walled nozzle for the isokinetic, super-isokinetic and sub-isokinetic flow conditions. The limiting streamline shows the flowline of the outermost gas particles which are drawn from the ambient stream into the inlet. For non-isokinetic conditions particles above certain limits may not be able to follow the curved limiting streamline due to the inertial forces. Therefore particles with sufficient inertia to escape the streamlines may not be sampled representatively. This leads to over-sampling of larger particles in sub-isokinetic sampling conditions and under-sampling of larger particles in super-isokinetic sampling conditions. Equations for the aspiration and transmission efficiencies belonging to each condition have been experimentally determined and can be found in Appendix B. Achieving iso-kinetic sampling conditions can be challenging and may also be hard to verify. Using equation 5.3, insight in the effect of a non-isokinetic sampling situation can be obtained.

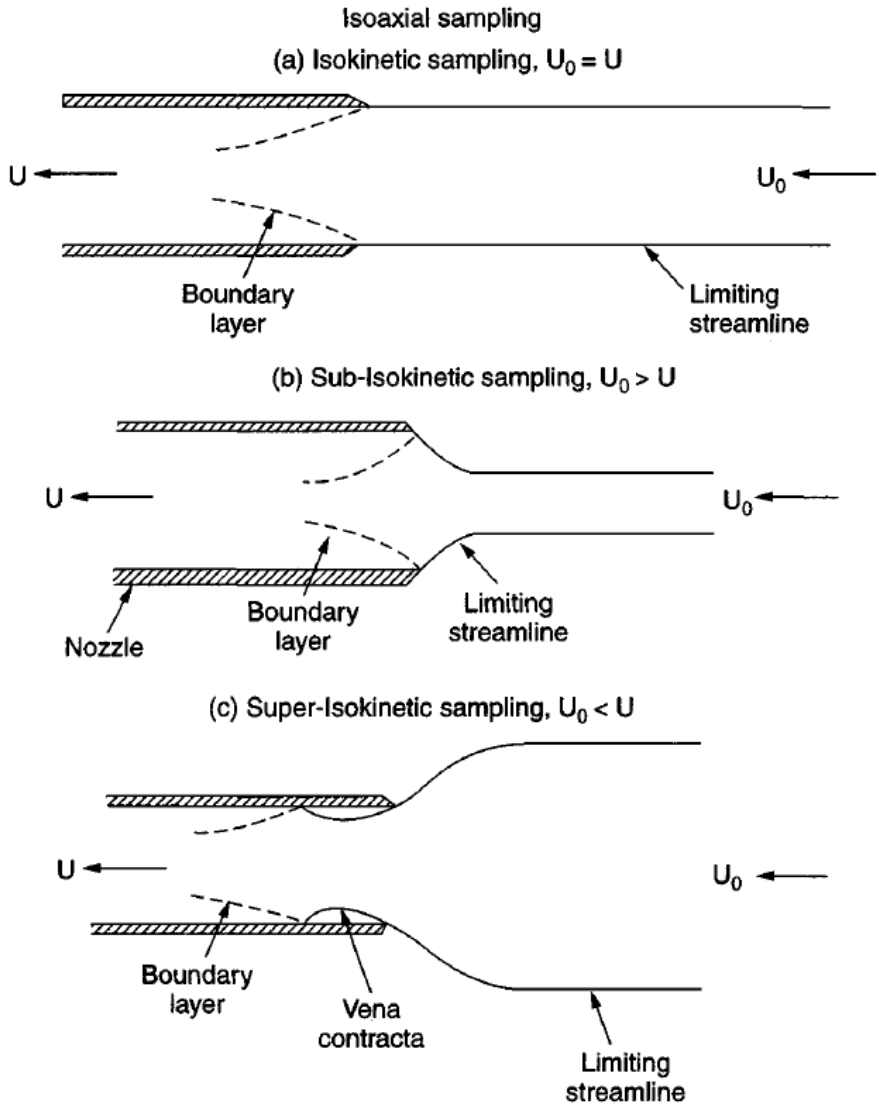

Figure 5.1: Schematic of isoaxial sampling with thin walled nozzle. The flow characteristics for (a) iso-, (b) sub and (c) super-kinetic sampling conditions are displayed. obtained from Aerosol Measurement: principles, techniques and applications, 2nd edition ,A Baron and K. Willeke, Wiley Interscience, 2001

[5]

5.2.2 Transport and mechanisms inhibitive to sampling efficiency

Apart from the issues of sample extraction, several factors can be identified which may impede the sampling performance in the process of transporting aerosols to a measurement device. This can be of influence on the sampling performance depending on the particle geometry and weight. Due to increasing gravitational and inertial forces that act upon the aerosol particles, it is generally more difficult to sample heavier particles. At the other side of the spectrum, smaller particles are more easily lost to the walls due to an increase in diffusion rate

The transport efficiency can be expressed as the product of the efficiencies of all the mechanisms involved with all flow elements.

$$\eta_{transport} = \prod_{flow_elements} \prod_{mechanisms} \eta_{flow_element,mechanism} \tag{5.4}$$

A lot of factors are involved in transport sampling efficiency. The list of (also previously mentioned) important mechanisms for water aerosol sampling is listed below, each behaving differently at various flow elements like bends and flow constrictions.

1. Gravitational settling
2. Diffusional deposition
3. Turbulent inertial deposition
4. Inertial deposition in (bends, flow constriction)
5. Particle re-entrainment after deposition

Approximation of losses in a bend based on stokes drag force
Every particle in a flow is subjected to aerodynamic drag. The amount of drag depends on the particle cross-section and the viscosity of the gas. Aerosols therefore have a tenancy to follow the surrounding gas flow. Without the influence of any forces a particle will perfectly follow the streamline of the flow it is on. The stokes drag force F_{drag} indicates the amount of force needed to achieve a certain relative motion between the particle and the surrounding gas. The stokes drag force is given by[5].

$$W = 3\pi\eta d_p (U - U_0) \tag{5.5}$$

η is the fluid viscosity, U_0 is the ambient flow velocity, U is the particle velocity and d_p is the particle diameter. In radial direction the general flow velocity can be approximated as zero and therefore be omitted from the equation.

In radial direction of a bend, an aerosol will experience centrifugal force and a resulting drag force in opposite direction. A balance will almost momentarily be realized within the bend length, as characterised by the particle relaxation time τ. This results in

$$m \cdot a = m\frac{U_s^2}{r} = 3\pi\eta d_p U_d \tag{5.6}$$

which can be rewritten to U_d, the drift velocity where r is the distance from the center of the bend to ther particle and m is the particle mass. Refer to Figure 5.3.

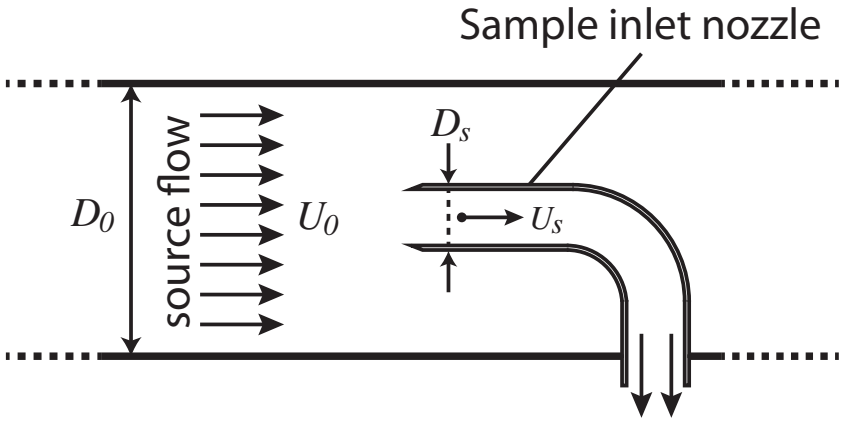

Figure 5.2: A schematic representation of a iso-axial sampling setup.

Now τ_{flow} is defined as the time needed for a particle to pass the entire bend. x_{drift} is defined as the largest drift from the entering radius when the bend is passed through. In this case we asses a quarter bend:

$$\tau_{flow} = \frac{2\pi r}{4}\frac{1}{U_s} \tag{5.7}$$

The drift speed multiplied by the time duration of the particle inside the bend gives the total drifting offset x_{drift} at the end of the bend.

$$x_{drift} = \tau_{flow} U_d = \tag{5.8}$$

The inertial efficiency in the bend is defined as the total amount of particles entering the bend over the amount of particles that are deposited. Assuming a homogeneous distribution, the cross-section surfaces surfaces representing the total and the drifted particle group can be used instead (Figure 5.3) A_d/A_{tot}. With known x_{drift} and D_s, the exact answer to this equation with known geometry leads to:

$$\eta = \frac{A_d}{A_{tot}} = 1 - arccos\left(\frac{x_{drift}}{2D_s}\right) \tag{5.9}$$

Substiting x_{drift} and D_s gives

$$\eta_{bend,inert} = 1 - arccos\left(\frac{\pi\rho d_p^2 U_s}{72\mu D_s}\right) \tag{5.10}$$

The result suggests that the inertial efficiency of a bend does not rely on the bend radius but only on the diameter of the tube.

Expressions for inertial efficiency in bends
According to Crane and Evans (1977), the inertial efficiency in a bend $\mu_{bend,inertial}$ can be approximated with a simple equation.

$$\eta_{bend,inertial} = 1 - Stk \cdot \phi \tag{5.11}$$

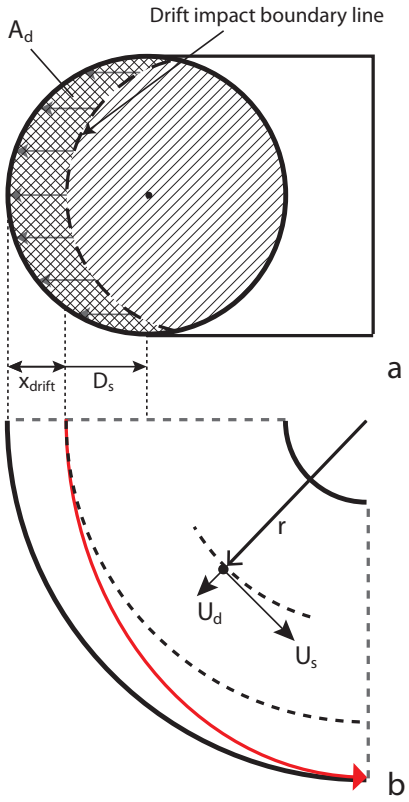

Figure 5.3: Inertial depositioning in a quarter bend.

Here ϕ is the angle of the bend in radians. This equation results in 100% efficiency only at a stokes number of 0 (Infinitly small particles). In reality this is not the case, especially in laminar flow from up to Stk 0,1 (depending on Reynolds number). Pui et al. (1987) have found a more accurate approximation based on experimental data for turbulent pipe flows:

$$\eta_{bend,inertial} = exp[-2,823Stk\phi] \tag{5.12}$$

Chapter 6

Experimental Setup

The experimental setup used to measure the water content in moist nitrogen gas flow consists of several separate components that are matched to function properly in conjunction. In this process, a maximal flow of 200 m^3n per hour is kept as guideline with a upper limit of 20 grams per m^3 of water content. For diagnostic purposes, an artificially generated sample flow is used to simulate different conditions. In this chapter the different components in both measurement setups are discussed, followed by the basic measurement routine that is used for all measurements.

6.1 Basic Measurement Outline

Roughly, the setup can be devided in two sections; sample generation and sample measurement. For the overall goal to determine the water content levels in a sample, a setup to measure the *mixing ratio* or *specific humidity* of moist gas sample is required. Additionally, to determine the accuracy of the measurements, the precise consistency of artificial samples that are generated have to be measured. Based on Equation 3.6 the sample generation section requires the following components to calculate the water content of the sample mixture that is generated:

- a droplet generator including a system to measure the amount of water that is released into the carrier gas
- a basic flow sensor to determine the carrier gas mass flow

In the measurement section, the specific humidity can be calculated using Equation 3.5, thus requiring:

- a relative humidity measurement probe for bulk mixture
- a temperature sensor in bulk mixture
- a pressure sensor in the measurement section

Since the specific humidity and mixing ratio measurements are only valid in gaseous conditions, heating is required to prepare the potentially moist sample mixtures for measurement:

- a heating system required to evaporate all possible liquid water in the carrier gas to prepare for measurement.

These ingredients are used in both the closed-chamber as the continuous measurement methods.

6.2 Experimental setup for discrete measurements

The closed system design is based on the idea that a captured gas volume, enclosed in an air-tight (impenetrable) chamber will hold its water content for later evaluation/measurement. This makes the measurement of the characteristics of the sample mixture straightforward because the characteristics are conserved. All time necessary can be taken to obtain measurement results.

6.2.1 The Measurement Chamber

Figure 6.1 shows a schematic representation of the measurement chamber used in the discrete measurement setup. It consists primarily of a sealable chamber made up of a regular pipe segment. Both ends can be opened and closed with ball valves. The chamber is fitted with two humidity probes, containing both a relative humdity sensor and a temperature sensor, a pressure sensor and additionally a wall temperature sensor for the chamber heating regulation. The entire chamber is encapsulated in a thick layer of thermal insulation to increase temperature stability and minimize the required amount of heating power.

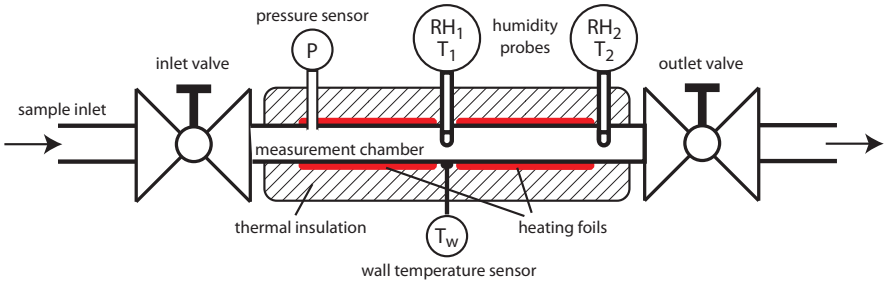

Figure 6.1: Heating tube schematic

Construction The measurement chamber is formed by a regular copper plumbing pipe section with an inner diameter of 26.5 mm and a length of 300 mm. The valves are connected with standard pipe fittings at either ends. The simple geometrical shape of the chamber ensures that dead spots in the encapsulated volume are avoided during gas flow-through. This design also minimizes the amount of protrusions in the flow that could cause accumulation of water droplets. The risk of capturing a mixture which is not representative for the incoming sample is minimized this way.

Humidity Probes Two 'General Electric MDR3' capacitive humidity probes provide the humidity measurements. This high end model has been chosen because for a number of reasons. Apart from high measurement accuracy and a factory calibration, this

RH measurement range	0 to 100% RH
RH measurement accuracy	2% (0-90% RH), 3% (90-100% RH)
Repeatability	$<$0,5%
Operational temperature	-10 to 85 $^{\circ}C$
Temperature measurement accuracy	$\pm$ 0,5 K

Table 6.1: GE MDR3 humidity sensor probe specifications

probe is easily interfaced with both humidity and additional temperature readout capability. Also the probe can handle high ambient pressures, a sufficient temperature range and has good recovery behaviour after being exposed to liquid water. Furthermore the sensor is encased in a sturdy probe which provides easy mounting options.

A schematic illustration is given if Figure 6.2. The probe consists of a long shaft with a sensor chip at the end. The chip contains both a humidity sensor as well as a temperature sensor for the determination of the relative humidity. The sensor can be covered with a screw-on filter cap to protect the sensor from debris. The shaft is made of stainless steel and design measures have been taken to thermally isolate the sensor from the probe shaft. The performance of the insulation barrier is not specified by the manufacturer.

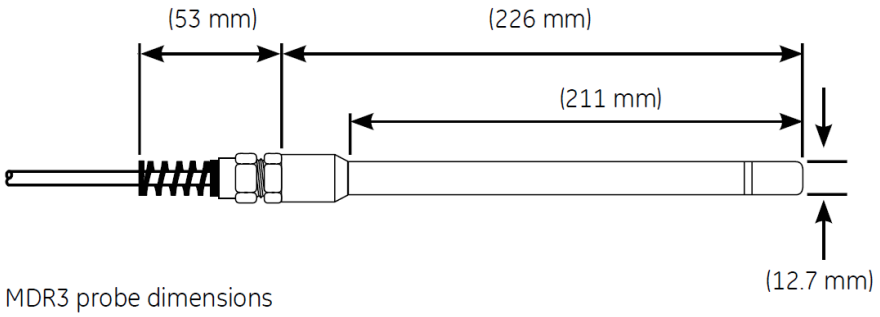

Figure 6.2: An schematic of a MDR3 probe with filter mounted. The actual sensor chip is concealed behind a removable filter cap.

The most important features are listed in Table 6.1. It is important to note that measurements at high humidity levels not only potentially cause ”clogging” of the sensor with water droplets but also results in lower accuracies according to the specifications. Measurements in this region must therefore be avoided. Operation also must be within the specified temperature range, requiring a temperature limit for the heating system.

The two humidity sensor probes used in the setup are fitted at the center and the far end of the measuring chamber tube. They are kept in place by an airtight nylon sleeve coupling which can be easily used to fit or remove the sensor. This construction has proven to be pressure proof up to at least 10 bar and temperature proof up to 80$^{\circ}C$. The depth of the sensor probes can easily be adjusted by sliding and fastening the shaft at the desired position.

The positioning at both the centre and end of the chamber are done due to 1) The measurements of both sensors can be compared to detect potential measurement errors in the case of large differences. 2) The placement of the sensors at different locations

in the chamber is done to asses the effect of the thermal leakage at either ends of the tube on the measured results. 3) The possibility of vertical mounting of the chamber can be investigated. The higher density of water vapour in comparison to nitrogen gas may cause a gradient in humidity as function of the height. By using sensors at the two locations in the chamber, this effect can be detected if it manifests itself.
Due to the fact that the sensor shafts are locked in place with the nylon sleeve couplings, the probe is in direct thermal contact with the chamber wall. The actual sensor however is at least to some extent thermally isolated from the shaft. Unwanted influences from the chamber wall temperature are therefore not likely but still potential faulty temperature readings that may result from this thermal contact form a possible source of error in the measurements. This matter can be taken into account when comparing the relative humidity measurement values of the two probes.

Heating System The heating power in the setup, used to increase the temperature of the captured sample and evaporate all liquid content, is delivered by 4 silicone foil heaters, evenly placed around the copper wall of the measurement chamber. These heaters each have a rated power of $100W$ at $230V$, providing a potential total heating power of 400 Watt. Using the heat capacity of typical sample, a heating rate of roughly $1°C$ per second can be reached with this amount of power in the ideal case. This is more than enough for this experiment. A rough estimation of the Biot number (Equation 4.1) for nitrogen gas in a cylindrical volume gives a Biot number of 10-100 depending on the conditions[1] This indicates that temperature gradients will be formed in the chamber at a constant wall temperature. The heating rate will thus be lower in practice.

The heaters are regulated with a temperature controller, and can be set to a certain temperature, using the chamber wall temperature sensor as reference. Approximately half of the entire outer surface area of the heating chamber is covered with the heating foils. Even so, the excellent thermal conduction properties of copper in comparison with the nitrogen bulk result in an even wall temperature at the axial center of the chamber. Thermal leakage at either ends of the chamber through the valves result in slightly lower wall temperatures at the ends of the chamber. This will inevitably lead to a lower gas temperature at the outer humidity measurement probe. Also, in the case of a low temperature and high water content, the colder surfaces near the valves are potential condensation spots. Ensuring that the wall temperature is well above the saturation temperature of the gas eliminates this problem.

6.2.2 Droplet generation and injection into carrier gas

The final measurement setup used in the current vortex tube setup, the primary or source flow coming from one of the vortex tube outlets is used as flow input for the measurement system. To simulate the operation conditions of the vortex tube, an artificial sample flow is generated using an *atomizer*.[2].

Six-jet Atomizer A liquid atomizer is used to inject a steady flow of liquid droplets of similar size into a passing carrier gas stream with six jets. Part of the droplets will evaporate virtually immediately until the gas approaches a saturated state. If the water

[1] The thermal conductivity of nitrogen gas is 0.026 W/mK (source: WolframAlpha). The convective heat transfer coefficient is dependant on flow conditions etc. and typically lies in the 10-100 w/m^2K range. The characteristic length of the system is the diameter of the cylindrical chamber.

[2] A device capable of atomizing water and injecting it into the carrier gas.

content is high enough, liquid droplets still remain and stay airborne. This results in the required moist nitrogen mixture exiting the unit. Six individual nozzles propel thin water jets onto spherical surfaces. A schematic representation of one nozzle situated in the atomizer unit is displayed in figure 6.3. The impact atomizes the liquid to a fine mist of water droplets of approximately 5 μm. An internal water reservoir feeds the jets using the pressure of the incoming gas. A pressure reducing valve is used to regulate the pressure of the jets. To regulate the rate of water droplet generation, the jet can set to the desired pressure. Each jet adds a similar amount of droplet content into the passing carrier gas. Any number of the jets, from zero to six, can be switched on simultaneously to easily multiply the droplet production rate. A bypass is available to dilute the mixture. The bypass is regulated with a valve and measured with a built-in flow meter. The bypass can be set from 0 to 80 litre per minute. To recreate a certain output from the atomizer, only the pressure and bypass have to be noted.

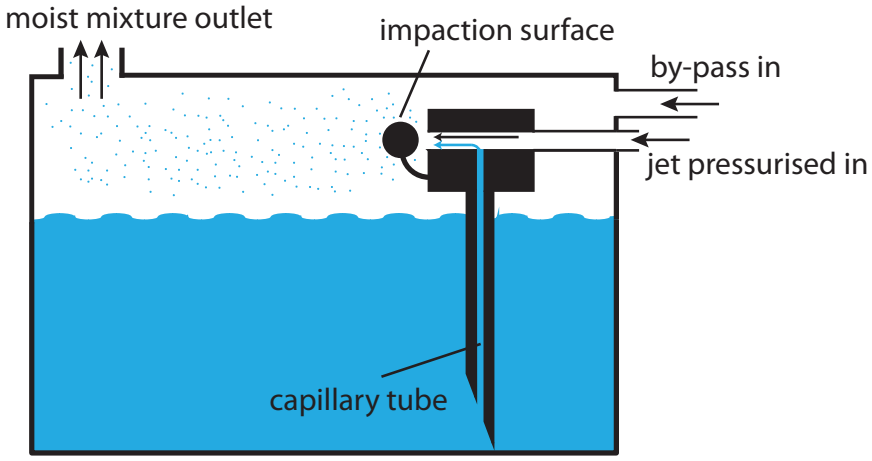

Figure 6.3: A schematic cross section of a nozzle inside the atomizer unit.

Atomization rate To verify the validity of the humidity measurements, an accurate determination of the water content in the generated sample mixture is essential. The six-jet atomizer lacks a precise measurement function for this purpose, so the entire unit is placed on an electronic scale to measure the weight of the water in the internal water reservoir as function of time. The mixing ratio of the generated sample can easily be determined using Equation 3.6 when the rate of water injection and the flow rate of carrier gas are known. An elaboration on this subject will follow in Section 6.4.2.

Operation and behaviour Summarizing the above, the following behaviour can be expected from the atomizer.

- The total gas flux is fixed if the jet pressure and bypass flow are set. This is independent of the gas input pressure as long as it exceeds the jet pressure setting.
- A linear dependency of reservoir water weight as function of time is expected when the jet pressure and bypass flow settings are maintained.

- Water content generation/atomisation is linearly dependant to the amount of activated jets.
- The droplet size distribution is narrow and around 5 μm

The atomizer does not behave ideally. The following factors may be of importance during operation:

- The average droplet size varies slightly with the jet pressure.
- Deactivating all vapour jets does not eliminate the carrier gas hydration entirely. A slight amount of water is transferred to the gas by evaporation from the reservoir. This may result in small deviations in the mixing ratio.
- The water level in the reservoir may (slighly) influence the water injection rate.
- Large agglomerated drops of water are ejected due to the combined effects of internal deposition and large gas flows at the exit nozzle.
- If that the capillary tubes are exposed to air in the case of low water levels, air bubbles may enter the tube and disturb the capillary function. This can cause unreliable varying water injection rates over time, for instance when a trapped bubble in a capillary tube reaches the top and the capillary working is lost.

6.2.3 Closed chamber implementation

In the implemented setup, the measurement chamber with the integrated heating system is connected directly to the atomizer as shown in the flow diagram in Figure 6.4.

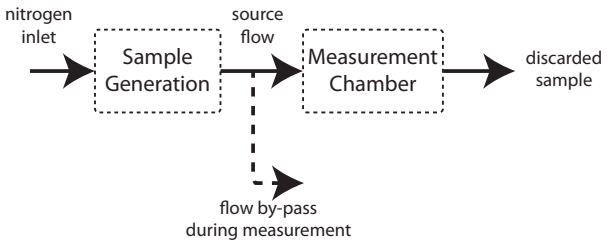

Figure 6.4: Schematic flow chart of the entire closed-chamber measurement setup.

The connection between the atomizer and the measurement chamber is kept short and smooth to ensure as little alteration to the 'generated moist gas sample mixture' as possible before the measurement chamber is reached. However, for convenience an equivalent of two 90° bends are needed.

1. Nitrogen Inlet": The nitrogen source providing the carrier gas is equipped with a flow sensor. The incoming nitrogen flow is measured for the carrier gas mass flow calculation
2. Sample Generation: Drops are injected into the nitrogen flow using the 6-jet atomizer. Adjustments can be made to simulate different measuring conditions.

3. Measurement Chamber: The sample mixture is led into the chamber and sealed. The built-in heating system is used to evenly heat the gas to the set temperature and evaporating all the liquid content that may be present in the gas. All available sensors are read out continuously during the process until a steady state is reached. A stable specific humidity indicates that no evaporation is taking place. A suitable chamber wall temperature with a sufficient margin above the saturation point of the enclosed mixture can be chosen depending on the expected water content.

6.3 Experimental setup for continuous measurement

The continuous measurement technique also relies on heating the sample mixture to increase the saturation point and evaporate all water droplets in the nitrogen flow. With the continuous measurement method a small sample from the primary flow is extracted and heated to a desired temperature. The relative humidity is measured in the same manner as in the closed chamber setup, by placing a sensor probe into the preheated and now non-saturated flow. The sampling procedure is required because the potential flow throughput could reach up to 200 m^3n, requiring a unnecessary high heating capacity in order to evaporate all the liquid water content. Apart from the sampling and and a specific heating solution, the continuous measurement setup can be used with the same measurement chamber, only now kept in a opened state.

6.3.1 Heating System

According to Fourier's law, Equation 4.1, providing sufficient heating to a gas with forced convection relies on the heating area, heating time and temperature difference between surface and bulk gas. Any combination will do as long as the gas has sufficient time to be heated. In other words, the heater must be able to dissipate it's heat into the gas flow. To increase the heating time, a tube heater solution is chosen with built in temperature regulator.

The heating tube consists of a resistive heating wire wound around a Teflon inner tube. A thick but flexible outer insulation layer prevents heat spreading to anywhere other than the inner tube. All is packaged in a flexible outer hose. A temperature sensor at one end of the tube is used to regulate the heating power to achieve a certain exit temperature. A thermal barrier is used so the heating coil is not in thermal contact with the temperature sensor.

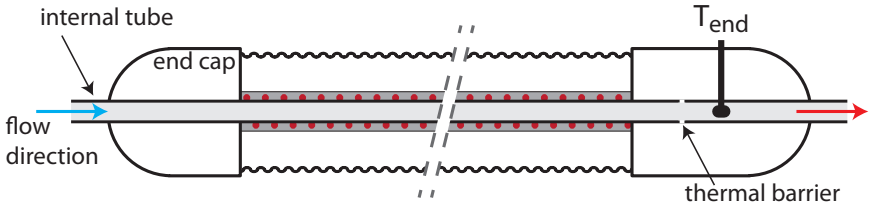

Figure 6.5: Heating tube schematic

Normal operation of the heating tube requires the temperature sensing side to be at the flow outlet. This way the outlet temperature is regulated. The manufacturer indicates that these types of heating tubes are designed to maintain fluid or gas temperatures in recirculating flow situations. The construction of the heating tube allows for a small difference in temperature between inlet and outlet flows and does not guarantee high temperatures throughout the entire tube. A numeric model is used to estimate the heating tube performance. More details can be found in Appendix C.

6.3.2 Sampling System

The sampling system as used in the continuous measurement setup is illustrated in Figure 6.6. The system consists of three parts: a sampling (inlet) tube, a sampling chamber section and a transition section to accommodate the incoming flow to the wider sampling chamber section.

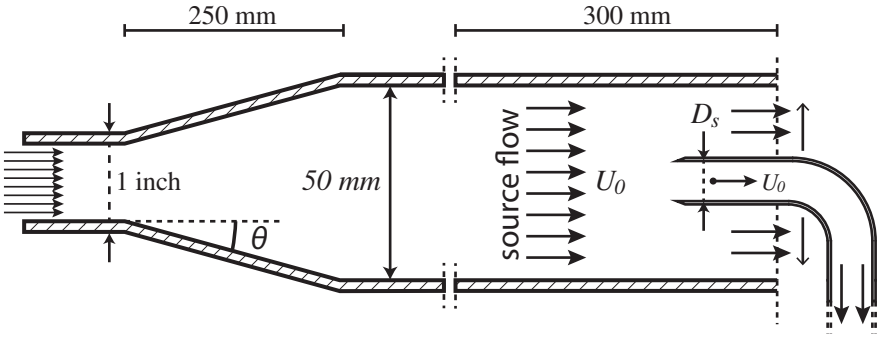

Figure 6.6: Sampling system schematic representation. The atomizer is directly attached to the entrance at the left side of the illustration. note: not to scale

Just like the closed-chamber measurement method, the atomizer is utilized to generate a moist nitrogen flow. In order to improve the sampling conditions, the atomizer outlet cross-section is increased to 50 mm with the transition section to both lower the flow rate and create more space for the sampling process. A maximal angle θ is used to avoid flow separation at the maximal expected flow rate (the final flow rate of the vortex tube (200m3n/h) has been taken into account). The sample chamber is used to capture the sample in developed turbulent flow conditions. The sampling inlet can be moved independently of the rest, so samples can be taken at different positions in the cross-section of the sample chamber. Three different sample tubes have been manufactured, with inner-diameters of 4, 6 and 8 mm. The radius of the quarter bend in the sample inlet tube is not of influence to the sample tube performance; only the sample tube radius and sampling speed influence the inlet efficiency (eq 5.10/5.11/5.12).

Transition from to a wider diameter before sampling is done to decrease the flow speed. This results in a more calm flow for better sampling and the decreased source flow speed also requires lower sampling speeds, which is more easily achieved. Since only the perimeter of the source flow will be influenced by the wall, losses due to depositioning and condensation will only affect these regeons initially. If the sample is extracted in the center region of the tube before the wall effects can mix with the rest of the source flow, the sampled mixture will be representative.

Creating iso-kinetic sampling conditions relies on source flow measurements and sampled flow measurements. A pump is placed after the measurement section to generate the required flow. Verifying that the correct sampling flow speed is used may forms a challenge and can not be directly observed with this setup. Only through calibration measurements with known source flow mixtures the sampling mode can be determined afterwards.

6.3.3 Implementation

In Figure 6.7 a schematic flow diagram of the total continuous measurement setup is displayed. The different components in the figure represent the previously described components of the setup. The components indicated with a red color form the sampling system. A description of the implementation of the different components in the setup is given below:

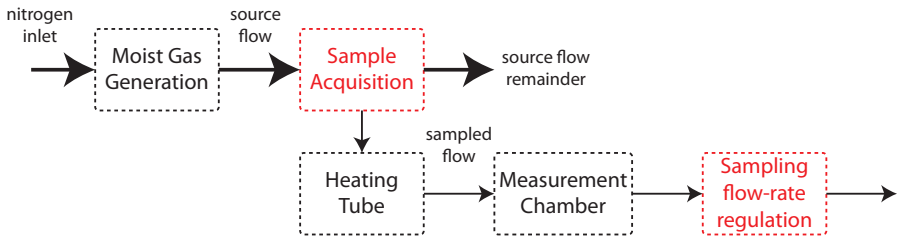

Figure 6.7: Schematic flow chart of the entire continuous measurement setup.

1. Sample Generation: Nitrogen source providing the carrier gas, incorporating a flow sensor. The incoming nitrogen flow is measured for the carrier gas mass flow calculation

2. Sample Generation: Drops are injected into the nitrogen flow using the 6-jet atomizer. Adjustments can be made to simulate different measuring conditions.

3. Sample Acquisition: A sample is extracted from the main gas-liquid flow isokinetically. This can be realized by adjusting the sampling speed to the main flow speed. The remainder of the source flow is discarded.

4. Heating Tube: The sampled flow is led through the heating tube, heating the gas and evaporating all the liquid content that may be present during the sampling process. The temperature output is adjusted to ensure total evaporation at the end of the heating tube.

5. Measurement Chamber: The heated gas is led to the measurement chamber in an open configuration. The sampled mixture should now be within the measuring window of the sensors.

6. Sampling flow-rate regulation: Generates a low pressure at the end of the measurement section. A constant flow at a certain pressure drop is achieved. A flow-regulating (throttling) valve is used to adjust the pressure drop, enabling an

adjustable flow rate to adjust to the sampling requirements. Flow rate measurements in the sample generation section and flow rate regulation sections are used to adjust the sample flow rate to the source flow rate.

The described setup has not yet been assembled at this point and no experiments involving sampling and continuous measuring have been conducted.

6.4 Measurement scheme

Only the measurement scheme for the closed-chamber method will be treated in this section, insufficient time was available to address the continuous method.

6.4.1 Closed Chamber measurement procedure

A strict procedure must be followed with each measurement for the sake of consistency. After some experimentation the following seems to achieve good results:

1. Set the chamber wall temperature T_w to the desired value.
2. Dry-heating and flushing procedure to eliminate any residual moisture in the chamber. Subsequently close the chamber until further use.
3. Tune the atomiser to the desired settings and turn on the flow.
4. Open the chamber and connect the atomizer outlet (loose fit so the tube is automatically decoupled when the chamber is closed and pressure starts to build)
5. Close the chamber inlet valve after a specific flow-through time t_f and close the chamber outlet valve one second later (to avoid pressure build-up in the chamber)
6. Measure for a period of 5-10 minutes depending on the expected evaporation period.

Because of the multitude of variables in the measurement process due to the number of different devices involved and the complex processes involved with droplet production and transportation, the setup is very sensitive to error. Every operation described above can produce varying results that can not be predicted depending on the precise execution.

Chamber dry-heating and flushing. Before each measurement, the chamber must be cleared of any water droplet leftovers that might still be present. The chamber can be dry-fired at a high temperature ($100^{\circ}C$) or flushed with dry nitrogen for a certain period of time to speed up the evaporation process. A combination of both is also possible. The result can be checked by closing the chamber and checking the relative humidity level, making sure it is approximately zero and does not rise much over time.

Data Acquisition and Processing All the measurement data is acquired with a one-second interval throughout the measurement process. All the data that is generated from the sensor values is stored in a single text file for each measurement. Only the pressure data is saved in a separate file due to the limitations of the separate sensor interfacing software.

A combination of Matlab and Origin is used to process all the acquired data. The primary objective is to calculate the specific humidity of the gas at any time during measurement so a development of the specific humidity as function of time is acquired. The result is compared with the expected specific humidity based on the sample production with the atomizer. A disadvantage of this method is that the specific humidity can not be calculated on the fly. This would be a great way of determining the state of the mixture. Without a direct SH calculation, the SH curve can only be determined after the measurement has ended, so relatively long measurement times are used just to be sure the mixture has stabilized.

6.4.2 Moist Gas production: Specific Humidity determination

The flow rate ϕ_{normal} of the pure nitrogen carrier gas is measured by a mass flow-meter in normal cubic meters (m^3n) per hour. For later use, this value is converted to a mass flow per second, ϕ_m by dividing by 3600 and multiplying by 1.25:

$$\phi_m = \frac{1.25}{3600} \cdot \phi_{normal} \tag{6.1}$$

The 1.25 factor arises from the conversion of normal cubic meters to kilos for the case of pure nitrogen gas. The water content that is injected by the atomizer per second is measured by the weight development of the entire atomizer. The mass of the entire atomizer (including reservoir) as function of time yields a linear relation, save the inconsistencies due to disturbances and settling behaviour. An example of such a relation, obtained from measurements is displayed in Figure 6.8.

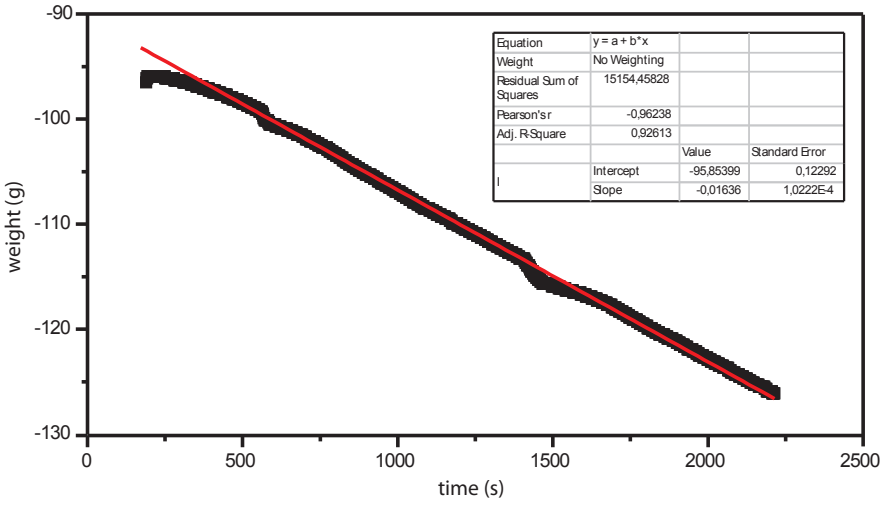

Figure 6.8: The atomizer mass as function of time as been output by the electronic scale. Only the relevant section of data is selected for fitting purpose. The red line represents a linear fit through the selected measurement data. Origin is used for the fitting process and calculates both a slope and the corresponding error.

Figure 6.8 shows a settling period of about 5 minutes. All scale measurement series

show this settling period, either from a higher or lower starting point. An explanation for this behaviour can lie in the fact that bending forces that are exerted on the atomizer by the connected pipes decrease in time until a steady state is reached. A slight disturbance is introduced two times in the measurement. Both times the weight curve recovers to a straight line. This indicates that the atomizer produces a constant water flux in time and that the measurement setup is able to recover after disturbances.

The slope of the fitted curve represents the water flux in g/s. For a linear fitting operation to succeed, only the relevant data point must be selected. Therefore this process is performed manually for each weight-development measurement using data-analysis software like Origin.

Division of the slope by 1000 gives the water flow ϕ_W in [kg/s]. The mixing ratio is obtained using Equation 3.6 and is convertible to the specific humidity using Equation 3.7.

$$r = \frac{\phi_W}{\phi_N} \tag{6.2}$$

A more detailed description of the involved calculations with errors can be found in Appendix D.

6.4.3 SH determination in the Measurement Chamber

For the specific humidity calculation in the measurement chamber using the sensor values, the data for RH, T and P must be obtained. Figure 6.9 shows a graph of the raw data obtained in a typical measurement.

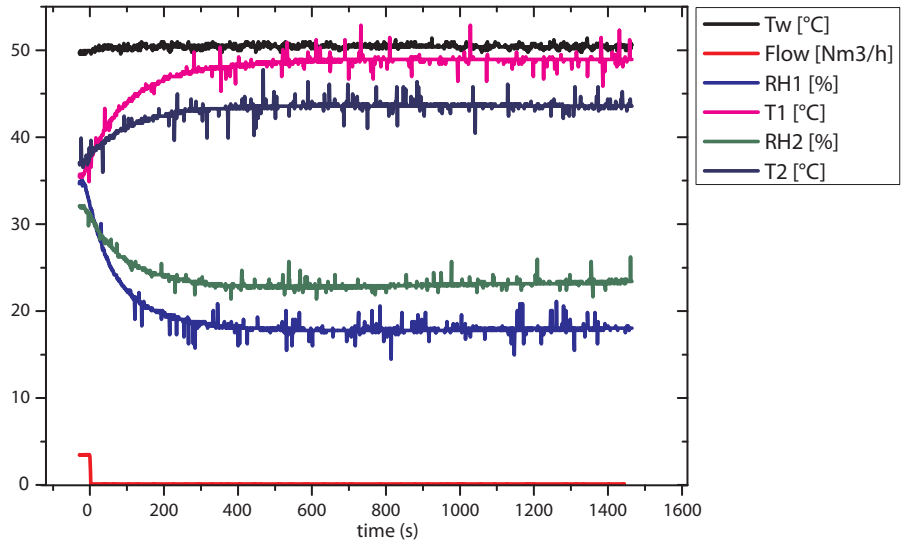

Figure 6.9: Graph of a typical measurement. Data from both humidity probes, wall temperature and flow speed are displayed. In this case a consistent mixture of moist nitrogen gas is led through the measurement chamber for 60 seconds. At $t = 0$ the valves are closed and the enclosed gas starts accommodating to the wall temperature of $50°C$.

A Matlab script is used to automatically import all the relevant files of a measurement series. Based on these datasets, a specific humidity is calculated as function of time. The manually processed values for the calculation of the expected water content in the chamber (as previously described) are entered separately, mass flow rate, weight slope with uncertainties. The results are combined and graphed as displayed in Figure 6.10.

All measurement values (fig. 6.10 a and b) are plotted for diagnosing purposes, and the results, including both the measured and expected specific humidity are combined as shown in fig. 6.10c. The dotted lines represent the outermost deviation from the expected SH value within its uncertainty range based on the atomizer weight calculations. More details on the Matlab script can be found in Appendix D.

Measurement Convergence Time Following from measurements like shown in figure 6.10, a certain stabilisation time can be defined for each measurement. The SH convergence time is the time needed for the Specific Humidity value to stabilize on the final value. Stabilisation of the specific humidity to a constant value indicates that the evaporation process is completed and the sample mixture is in the gaseous state. Figure 6.10c shows a convergence time of approximately 200s, even though the individual humdidity, temperature and pressure values displayed in 6.10 a and b require roughly twice that time to reach an equilibrium state. When the specific humidity stabilizes, it is safe to obtain the measurement value. A faster convergence time is obviously preferred to increase the measurement rate.

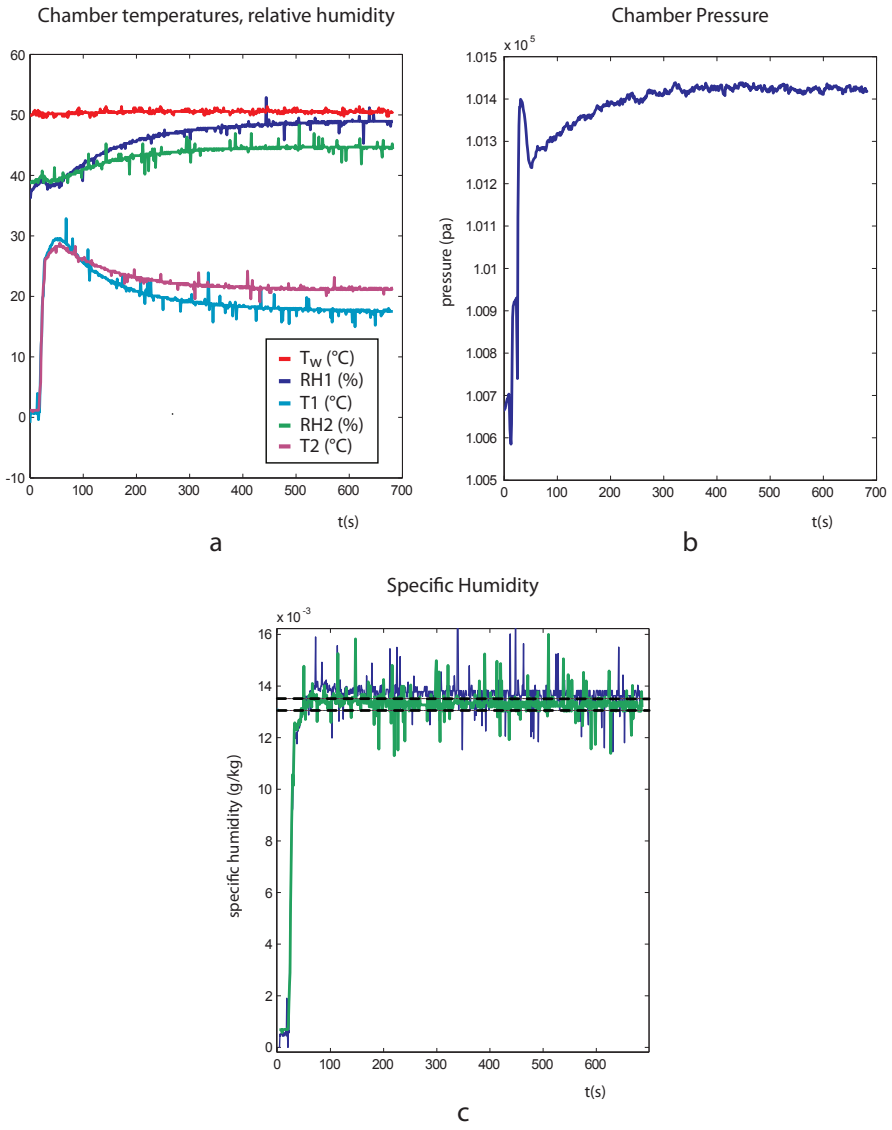

Figure 6.10: Matlab processing results of a single measurement.

Chapter 7

Measurement Results (and Discussion)

The results from the project follow from a range of observations and datasets obtained with multiple series of measurements. All measurements have been acquired using the closed-chamber measurement method. The majority of the measurements conducted are related to harmonizing the provided sample water content and the actual measured water content. Both the atomizer and direct water droplet insertion into the chamber have been used. During all measurements presented in this section, the same atomizer configuration was used: 3 jets where active during moist gas production with a jet pressure of 50 psi and a bypass of 40L/min. In practice, this configuration results in a moist gas with an SH of about 0.013-0.015 for the different measurements. The uncertainty in the SH arises from the fact that measurements results had some variations over time after turning the atomizer off and on again. For individual measurements, the output was however constant according to the weight graphs that all involved a linear dependency.

A sample of SH 0.014 has an saturation temperature of about 23 $^{\circ}C$. The output of the atomizer is about 10 $^{\circ}C$, resulting in a moist gas that is comparable to a typical vortex tube output. A measurement chamber wall temperature of 50$^{\circ}C$ is sufficiently high to ensure total evaporation of the liquid water droplets and is used in most measurements.

7.1 Measurement Quality

For a series of 10 consecutive measurements, the exact same conditions where created for each measurement to determine the measurement quality. The measurement quality is defined by the accuracy, resolution and precision of the measurements. The fine-tuned measurement scheme, mentioned in the experimental setup was used to achieve as much consistency as possible.

Measurement Resolution A single measurement of the closed-chamber setup is calculated using 3 sensors: a temperature sensor, a humidity sensor and a pressure sensor. The sensor values are acquired with a certain fixed resolution. This directly manifests itself in the SH calculation resolution. In figure 7.1, the specific humidity curve progression in time is displayed in exploded view of Figure 6.10c. The magnification

shows a clear development of the calculated SH values during a measurement as function of time. All measurements show a similar behaviour of the calculated SH curve.

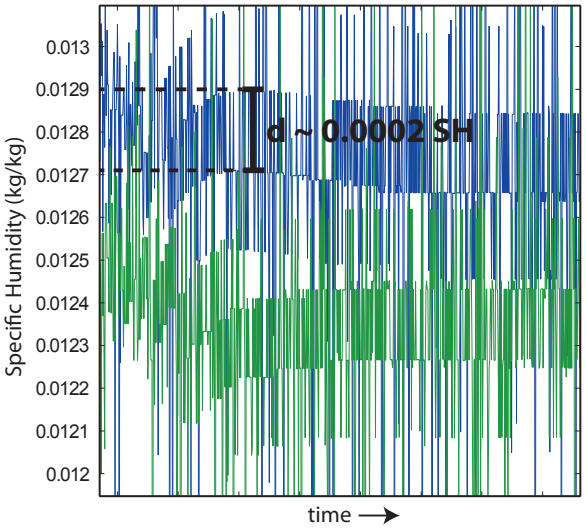

Figure 7.1: Measurement Resolution. An exploded view of a specific humidity graph to illustrate the maximal achievable read-out accuracy.

When carefully inspecting the graph, it becomes apparent that the SH value revolves around a certain value with a fairly constant resolution of the measurement. This rough 'step', denoted with d, can be clearly recognized in the graph. It has a size of approximately $0,0002 kg/kg$. This forms the resolution of the measurement and the read-out precision is limited by this. Small variations in resolution are seen for different conditions.

Measurement Accuracy The accuracy of the measurements is determined by the spread of a series of identical measurements. Since the individual measurement accuracy is limited by the previously described resolution, the spread in results are influenced by slight variations in droplet production, and the sample transport deposition and re-entrainment processes that may alter the sample in unpredictable ways. The result is displayed in Figure 7.2.

The calculated measurement results are scattered slightly around the expected SH value with a absolute uncertainty of about 0.0016 for both the probes. This equates to roughly 12% absolute deviation around the mean value for the used transport system and sample settings. The measurement accuracy of the center and side probe are as good as equal so no conclusions can be made regarding the preferable position at this point.

Measurement Precision A constant factor that returns in every single measurement is the fact that the measured specific humidity at the centre probe is always slightly higher than the SH that is acquired with the perimeter probe. This is the case for all measurements and indicates either a lower water content at the far ends of the chamber

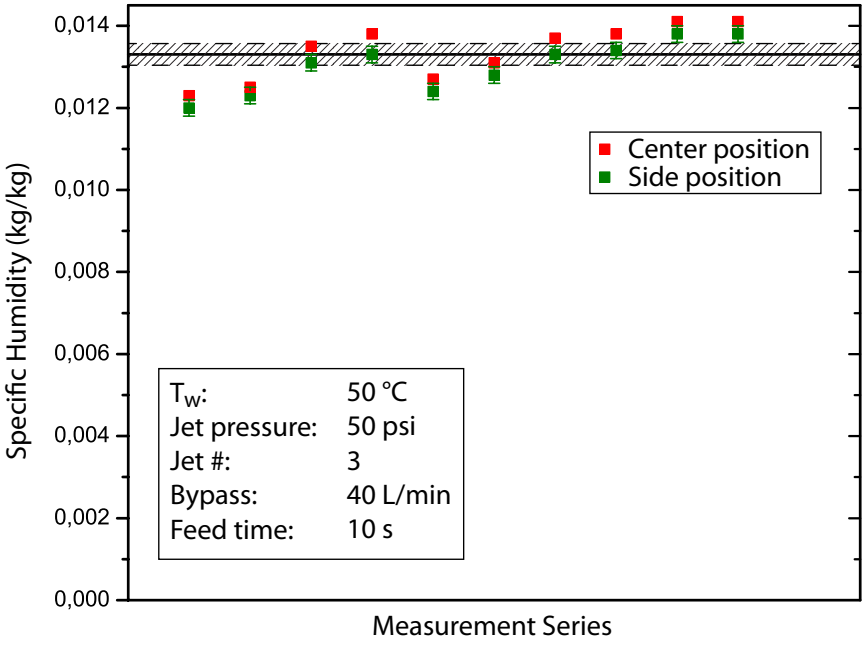

Figure 7.2: Measurement Accuracy Series

or a measurement error due to the temperature differences. At this point not enough results are available to rule out either of these potential causes. Therefore, a preference for which probe location (or perhaps a combination) to use is not pronounced at this point. Since the used moist gas generation method may include various uncertainties in output, no statements about absolute measurement precision can be given. A method to inject very precise amounts of water in combination with an accurate chamber volume might lead to a better gauging point to determine the absolute measurement precision.

7.2 Variation of Variables

Over the course of two days, several measurements where conducted to explore both the system response to temperature change and the response to varying feeding time. All measurements where conducted with samples using the same atomizer configuration. These measurements where among the first successful measurements, but lacking a fine-tuned measurement process that was developed in a later stage. This results in larger number of measurements with a more inconsistent behaviour.

Temperature Variation A series of measurements involving a variation of chamber wall temperature has been conducted. The results are displayed in figure 7.3

As indicated, not all measurements where equally successful[1]. For instance none of the 30 $°C$ measurements succeeded. When disregarding the 'faulty' measurement

[1]This is partly due to the fact that these measurements where conducted at an early stage in the experiments, where the measurement procedure was not yet optimized.

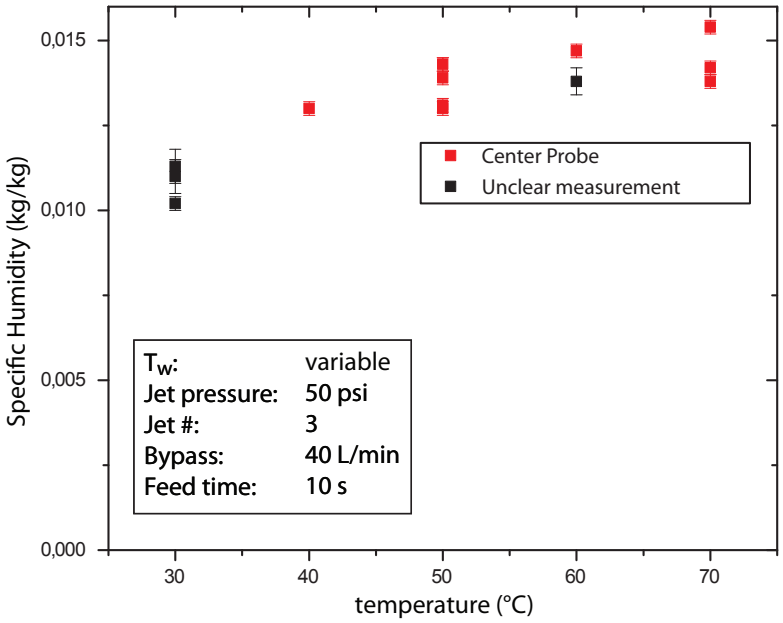

Figure 7.3: Measurement result as function of the chamber wall temperature

points, seen in Figure 7.3, a clear dependency of measurement result on the chamber temperature can not be confirmed. The lower values for lower wall temperature can be an indication of a region of condensation, for instance on the relatively cold valves. The deviations in measurement that where found earlier in the accuracy series, return in these results. These deviations dominate any potential dependency on the wall temperature so no final conclusion can be made. Also, the measurement readout accuracy (displayed with the error bars) also does not show any apparent dependency on the wall temperature.

Measurement Convergence Time An exponentially decreasing dependency of the convergence rate on the chamber temperature was found based on the measurements of Figure 7.3. With the same sample configuration that is used in all the previously covered measurements, a very consistent period of about 200 seconds was needed at 50 $^{\circ}C$ before the final SH could be obtained. At 70$^{\circ}C$ the required time decreased dramatically to only 40s (based on 1 measurement). The stabilisation time at 30 $^{\circ}C$ proved to be excessively long, and was not reached once during any measurement. Of course, changing the sample mixture will also change the convergence time. In general, higher temperatures are preferred in order to increase the measurement rate without any apparent loss in accuracy.

Feeding Time Variations Similar to the previous, the feeding time of sample mixture through the chamber was varied. The results are displayed in Figure 7.4. Considering the previously found measurement deviations, the results suggest no dependency of the measured SH as function of the feeding time from 10 seconds to 60 seconds. Measure-

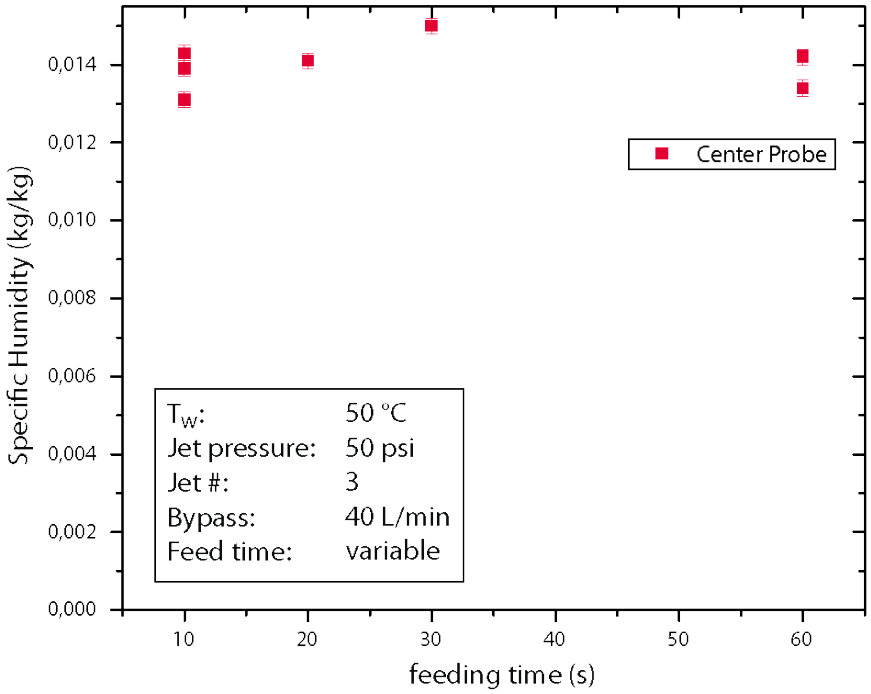

Figure 7.4: Measurement result as function of feeding time

ments involving different mixtures not been performed.

7.3 System response to direct liquid water injection

To assess the spreading speed of water vapour inside the measurement chamber, a single droplet of water is placed inside the measurement chamber after completely drying the chamber. The droplet is placed directly under the the central humidity sensor.

The effect of direct water droplet insertion into the measurement chamber provided interesting insights in the reaction of the characteristic measurement parameters as function of time, based on a localized evaporation process. To illustrate the process with the most detail, a low temperature is of 30 $^{\circ}C$ is set for the chamber wall. A single water droplet of $5\mu L$ in the preheated chamber containing only dry nitrogen gas results in the measurement set displayed in figure 7.5.

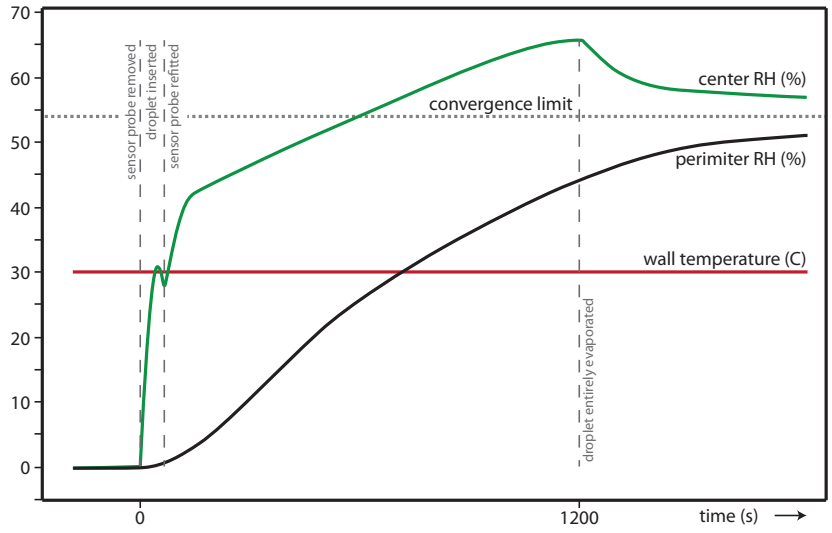

Figure 7.5: The effect of a $5\mu g$ water droplet on a measurement in the closed chamber. The droplet is placed in close proximity of the centrally placed humidity sensor (RH1).

The green line, indicating the center humidity sensor measurement curve, shows a immediate and almost linear reaction to the evaporating droplet. The black line which shows the relative humidity at the far end of the measurement chamber, shows a delayed reaction to the droplet. This is due to a lack of convection in the thermally settled system, resulting in a situation where diffusion is the only spreading mechanism. After a 20 minute period a collapse of the centre RH occurs, indicating that the droplet is entirely evaporated. From this point on, diffusion causes the relative humidity at the centre and far end of the chamber to slowly converge to approximately 54%. This first attempt does not have the accuracy to give precise measurement results in terms of absolute SH values. However, concluding from the slow spread of water vapour in the chamber, a non-homogeneous state of the mixture could be the cause of the slight difference in SH values that are obtained from the measurement probes.

By optimizing this injection method, the precision of the measurement method can be determined by excluding deviations due to sample generation and sample transport.

7.4 Preliminary Results of Tube Heater Performance

Preliminary measurements have been conducted to assess the heating tube performance. A combination of the closed chamber measurement method and the continuous heating method are combined by preheating the sample flow with the heating tube before it is captured in the measurement chamber. The first results obtained with this setup indicate that substantial amounts of water accumulate inside the heating tube due to it's design: The heating tube can only only regulate out-coming flow temperatures and *not* the wall temperature throughout the tube. With the heating power evenly distributed over the tube, low wall temperatures can arise in the inlet section of the tube due to the cold in-flux and relatively high evaporation rate. This results in condensation and further accumulation of water inside the tube even though the flow that exits the tube is heated to requirement and fully evaporated. As this setup closely resembles the definitive sampling setup, this problem must be addressed in order to achieve good results with the continuous measurement method. Further experiments must be conducted to determine the extent of this problem and methods to resolve this issue.

Chapter 8

Conclusions

Regarding the initial mission statement, the following conclusions can be made following from the conducted experiments and advancing insight.

- The closed-chamber measurement experiments resulted in consistent measuring results. Even though variations can be seen in results with the same moist gas production settings, this only seems to be due to slight variances in the produced sample and not a result of measurement error. No signs of unexpected behaviour of the measurement results where found within the measurement accuracy.

  A more precise approach for determining measurement precision of the closed-chamber method must be developed to eliminate small sample generation variances and eliminate sample transport effects that alter the sample mixture before it reaches the measurement device.

  The closed-chamber method seems to be feasible for implementation in the final vortex tube setup. Although only discrete measurements can be obtained using this measurement method, the measurement frequency can be limited to a couple of minutes when using the right measurement settings.

- The continuous measurement method has not been implemented yet. However, preliminary experiments with the presented continuous heating solution has proven to be unsuited in the current application. Condensation at the beginning section results in water aggregation in the heating tube. The heating tube can however be used for sample transportation of pre-heated sample flows without deposition losses. Compared to the closed chamber measurement setup, a lot of extra complexity is added in the form of a sample extraction process and a continuous flow heating process. At this point it seems that the added complexity will only negatively influence the measurement result. However, this does not eliminate the continuous measurement method as a suitable alternative. Experiments with the continuous measurement setup must first be conducted before any definitive conclusions can be made.

  Two main challenges are expected regarding the continuous setup. The first challenge involves the sampling process. It will be challenging to determine if a proper sample mode is achieved and a method must be developed to determine this. Without the possibility to verify iso-kinetic sampling mode, it is uncertain if a representative sample is acquired from the source flow. The second challenge

involves sample transportation to the measurement section. Eliminating all deposition and condensation spots in the entire flow path of the sample will be of great importance.

8.1 Recommendations

The following section is used to give suggestions for further improvement of the measurement performance of both the closed chamber and the continuous measurement setup.

Closed-chamber improvements Improvements to the closed chamber measurement device can be achieved mainly by including the valves in the heating zone. This eliminates any potential temperature gradients and possible condensation points throughout the chamber.

For precision measurement purposes, a very precise droplet depositioning device with the ability to inject a specific amount of water without the requirement to open the chamber will be of great benefit. With this approach, any uncertainties involving moist gas production and sample transport are eliminated.

Continuous method improvements Even though the continuous setup has not been tested yet, a couple of improvements can be though of when considering the sample acquisition and transport:

1. During moist sample transport over long distances, use tubes with heated walls to limit condensation effects.

2. The sampling inlet tube has a 90 degree turn in the current design. This bend (with the associated inertial depositioning effects) can be eliminated by keeping the sample tube straight. Instead the residual source flow after the sampling tube can be bent away.

3. To minimize condensation and turbulent deposition effects in the sample tube, the sample tube can be heated to high temperatures. One approach is to construct the tube from a thin metal foil which can be heated directly by imposing a current.

4. An alternative heating method like microwave coupling directly into the water vapour and liquid droplets might be a good solution to quickly evaporate any droplets in a short section of plastic tubing.

Bibliography

[1] *Physical Properties Table*, Antoines Equation, source unknown.

[2] *Comparison of the Antoine equation and a 3-term Chebshev equation for correlation of vapor pressures*, Walter N. Trump, Computers & Chemistry Volume 4, 1980 pages 117-122.

[3] *Investigation of Aerosol Aspiration by photographing particle tracks under flash illumination*, Belyaev and Levin, Journal of Aerosol Science, March 1972

[4] *Techniques for collection of representative aerosol samples*, Belyaev and Levin, Journal of Aerosol Science, August 1974

[5] *Aerosol Measurement: principles, techniques and applications, 2nd edition*,A Baron and K. Willeke, Wiley Interscience, 2001

[6] *Glossary of Meteorology, 2nd edition*, American Meteorological Society, electronic version

[7] *WMO Guide to Meteorological Instruments and Methods of Observation - 7th edition*, chapter 4, World Meteorological Organisation, August 2008

[8] *WolframAlpha knowledge database*

[9] *Choosing a Humidity Sensor: A Review of Three Technologies* - K.Roveti, Sensor Magazine, July 2001

[10] *Heat Transfer: a practical approach, 2nd edition* - Cengel and Yunus, McGraw-Hill, 2003

[11] *Engineering Heat Transfer, 2nd edition* - William S. Janna, CRC press, 2000

Appendix A

Humidity Measurement Sensors

Three types of solid state humidity sensors are on the market today, offering solutions for a variety of applications. The solid state sensors, unlike a lot of analogue measurement devices, are ideal for scientific research applications because of the small form-factor, easy and continuous electronic read-out, remote operation and durability. It is essential to choose the right sensor for the right job. The three sensor types discussed below [7][9]:

A.0.1 Capacitive humidity sensors

Capacitive humidity sensors use the effect of water molecules on the dielectric constant of a polymer layer to detect humidity levels. The polymer layer is sandwiched between two electrodes, forming a capacitor. Due to the strong dipole moment of water molecules, a altered ambient humidity results in a small capacity change. The small nominal capacitance of well below a microfarad requires an excitation frequency of several kilohertz to measure the impedance of the sensor. Therefore a connection to the measuring electronics proves to be problematic with long wire leads. This is why the measuring electronics of capacitive sensors are usually integrated in the sensor head, making it necessary to consider the effects of environmental conditions on the electronics. A well designed sensor with good sensor interface is corrected for such factors and therefore performs well over a wide range of conditions, (pressure, temperature, humidity).

Capacitive humidity sensors can typically measure the relative humidity in a range of 5-95 percent relative humidity. The accuracy of such measurements lies within the 2 percent accuracy range when the sensor is appropriately calibrated either in factory or on-sight. Sensors with no calibration have an accuracy that is up to 3 times lower than the calibrated counterpart. Capacitive humidity sensors are not very sensitive to contamination and temperature changes, are fairly resistant to chemical vapours, operate at high temperatures (up to 200 °C) and requires little maintenance. Combined with the flexibility of remote sensor placement makes this a widely used sensor in industrial-, commercial- and weather telemetry applications.

A.0.2 Resistive humidity sensors

Resistive humidity sensors use the resistance variance in certain materials with respect to ambient humidity levels. Only the surface layer of the sensor is sensitive to changes

in humidity, making that this type of sensor responds very quickly to changes in humidity. The direct current resistance is measured over the sensor unit, changing polarity with a low frequency to avoid polarization. Resistive humidity sensors have an exponential response, thus requiring analogue or digital signal conditioning circuitry to linearise the signal.

Resistive sensors are typically very basic sensors, requiring only simple electronics for signal interfacing, easy one-point calibration resulting in accuracies of 2 percent relative humidity. Resistive sensors perform better in lower temperature ranges from $-40°C$ to $100°C$

A.0.3 Thermal conductivity humidity sensors

Thermal conductivity humidity sensors are, unlike the majority of humidity sensors, used for the measurement of *absolute humidity* directly. This type of sensor measures the ability of the air to conduct heat which is measurably influenced by the humidity level. The thermal conductivity humidity sensor consists out of two identical thermistors of which one is encapsulated in nitrogen gas and shielded from the environment while the other is exposed. Each resistor receives an identical current, heating the units to over $200°C$. The difference in final temperature indicate the humidity level of the environment.

Absolute humidity sensors operate at very high temperatures up to $300°C$. Typically the accuracy lies in the vicinity of $3g/m^3$. This implies a higher accuracy expressed in relative humidity at higher relative humidity conditions. Reliable measurements can be taken with the thermal conductivity technique up to the saturation point of the air because the condensation process acts as a heat sink and disrupts the operation of the unit. However, regeneration ability of the sensor after over-saturation is very good and takes place rapidly due to the fact that the heated elements accelerate evaporation.

In general the sensors are very durable, only require one-point calibration (zero-point calibration in dry air or -nitrogen) and are very resistant to chemicals when inert materials such as glass are used for construction.

Appendix B

Sampling Efficiency

Equations for aspiration and transmission efficiencies in a sampling situation for thin walled sampling inlets are summed up in the following section. When the sampling speed and the source flow speed are known, the inlet efficiency can be calculated using Equation 5.3.

$$\eta_{asp} = 1 + \left[\frac{U_0}{U} - 1\right]\left[1 - \frac{1}{1 + k \cdot Stk}\right] \tag{B.1}$$

Where $0,18 \leq Stk \leq 2,03$ and $1,17 \leq U_0/U \leq 5,6$.

$$Stk = \frac{\tau U_0}{\delta} = \frac{d_p^2 \rho_p U_0}{18\eta\delta} \tag{B.2}$$

$$k = 2 + 0.617\left[\frac{U_0}{U}\right]^{-1} \tag{B.3}$$

$$\tau = \frac{\tau U_0}{\delta} = \frac{d_p^2 \rho_p}{18\eta} \tag{B.4}$$

δ is the pipe diameter. The Stokes number indicates the stopping distance of the particle in relation to the characteristic dimension of the flow geometry. Effectively it is a measure of how quickly a particle can adapt to a change of flow direction. Particles that can easily accommodate to changes in the flow direction have a Stokes number smaller than 1.

Inertial transmission efficiency for isoaxial sub-isokinetic sampling conditions for $(0.02 < Stk < 100)$ and $(1 < U_0/U < 10)$:[1]

$$\eta_{transmission,inertial} = \frac{1 + \left[\frac{U_0}{U} - 1\right] / \left[1 + \frac{2,66}{Stk^{2/3}}\right]}{1 + \left[\frac{U_0}{U} - 1\right] / \left[1 + \frac{0.418}{Stk}\right]} \tag{B.5}$$

Inertial transmission efficiency for isoaxial super-isokinetic sampling conditions for $(0.02 < Stk < 4)$ and $(0.25 < U_0/U < 1.0)$:[2]

$$\eta_{transmission,inertial} = exp[-75I_v^2] \tag{B.6}$$

[1] (Liu et al,1989)[5]

[2] (Hangal and Willeke, 1990b)[5]

$$I_v = 0.09 \left[Stk \frac{U - U_0}{U_0} \right]^{0.3} \tag{B.7}$$

$$\eta_{transmission,gravitational} = exp \left[-4,7 K_\theta^{0,75} \right] \tag{B.8}$$

$$K_\theta = Z^{1/2} Stk^{1/2} Re^{-1/4} \tag{B.9}$$

Appendix C

A Numeric Heat Transfer Model for pipe flow

C.0.4 Numeric Heating Model

In the case of moist gas, containing both water vapour and liquid droplets, the heat capacity of the carrier gas, water vapour and liquid water must be considered. The phase transitions must also be taken into account. As a result the distribution of the gas and liquid phase components of the water content in the carrier gas change continuously throughout the heating process. In the liquid to gas transition a certain amount of energy is extracted from the environment, where the speed depends on the rate of condensation.

To approximate the time needed for a moist gas mixture to heat from a specific temperature T_i up to temperature T_f, the energy balance of all the above factors must be considered. The precise progress of the phase transition and heat distribution is too complicated to model exactly, so a couple of assumptions and approximations are made for the gas involved:

1. The gas components in the mixture are ideal in the sense that:
    - the heat capacities of the different components in the system do not vary with the temperature
    - The heat capacity of the gas/liquid mixture is approximated by adding the separate heat capacities of the different components. (in practice the heat capacities may not be taken separately because the mixture of components form a slightly different value)
2. The mixture of nitrogen, water vapour and water droplets is homogeneously distributed in the heating chamber.
3. The water droplets in the mixture are small enough to stay airborne and no accumulation of water occurs at the bottom of the chamber
4. The evaporation speed is infinite (this is valid for infinitely small liquid droplets, forming an infinitely large evaporation surface). As a result, the moist gas mixture will always be saturated until all the droplets are evaporated

Heat transfer from a heated pipe to the internal gas flow poses a challenge as there is no direct formula to calculate the heating performance. To accommodate the tube heater to the rest of the setup, a numeric model is used to calculate the expected performance. For dimensioning purposes the heating power of the tube must be calculated as function of the heating tube specifications and gas flow speed through the tube. In this situation *forced convective heat transfer* is the main mode of heat transfer from the heating coil to the gas flow. Fourier's law of Equation 4.1 shows that heat flux in such a situation is linearly dependant on the temperature difference between the bulk gas and the tube wall. Using the heating tube in a heating situation implies a substantial temperature difference between entrance and exit of the tube. The entrance will be approximately the same temperature as the gas temperature before heating. Once a steady-state has been reached the gas temperature at the end of the tube will have reached the set value. A temperature gradient will form throughout the tube wall in axial direction, causing a uneven distribution of heat flux into the gas flow along the tube axis. In the colder area at the beginning of the tube the large temperature difference implies a larger heat flux as opposed to the end of the tube where the now heated gas results in lower heat flux. Taking into account the temperature gradient in the tube, caused by a gradually heated gas mixture, the beginning of the heating tube will be much colder than the end of the tube.

A numerical model of the system is introduced using discrete length intervals to determine the heat flux to the bulk gas flow and the resulting temperature development throughout the heating tube. All is based on the forced convection heat transfer mode and Newtons cooling law that can be used to describe it. Figure C.1 is used to describe the numerical model in the following section.

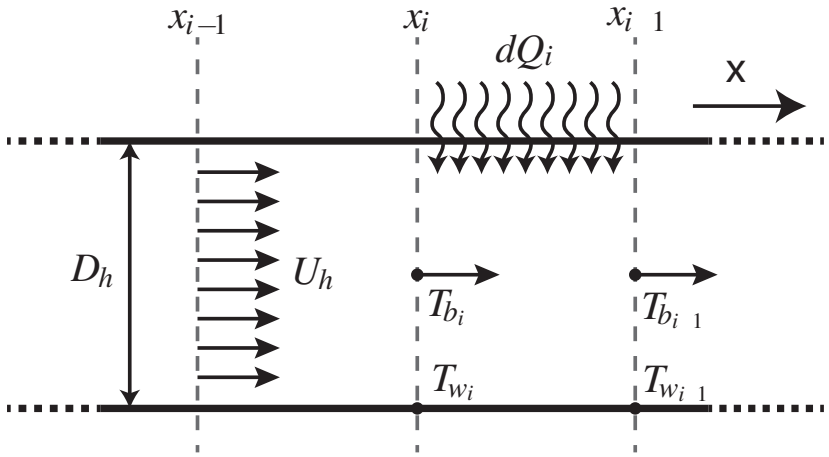

Figure C.1: The numerical model is based on discrete steps in the heater tube.

The lack of further specifications forces the use of some assumptions. Only the maximum power of the unit is specified, together with the inner tube diameter and length of the tube. For convenience the heat flux per unit surface area q'' is approximated as a linear function of the temperature difference between bulk T_b and wall T_w.

Two calibration points $q_1''$and q_2'' at wall temperatures T_1 and T_1 are needed. (Refer to Figure C.1)

$$q_i'' = q_1 - \frac{(q_1'' - q_2'')}{T_2 - T_1} \cdot \left(T_{w,i} - T_{b,i}\right) \tag{C.1}$$

To calculate the tube temperature, bulk temperature, heat flux per unit surface area and the heat transfer coefficient h are used. Rewriting Newtons cooling law and implementing the discrete system gives

$$T_{w,i} = q_i''/h + T_{b,i} \tag{C.2}$$

The heat transfer coefficient can be calculated with Equation 4.5. The change in bulk gas temperature from step i-1 to step i can be calculated using equation xx. In this equation, basically the effective heat used for heating (substracted the heat used for evaporation of liquid droplets) is divided by the heat capacity of the passing gas.

$$\Delta T_i = \frac{\left(dQ_{h,i} - dQ_{vap,i}\right)}{(1/4) \cdot \rho \cdot \pi C_p \cdot D_{tube}^2 dx} \tag{C.3}$$

where $dQ_{h,i} = A_i \cdot q_i''$ is the amount of energy transferred to the bulk in section i, $dQ_{vap,i} = Q_{vap} X_{sample}/981$ is the amount of heat used for evaporation in section i, and the denominator describes the heat capacity of the matter in section i. dx is the length of a section i and is equal to $x_i - x_{i-1}$. 981 is the number of sections in which the entire tube is divided. The evaporation heat Q_{vap} for water is approx. 2250 kJ/kg. Because it is very hard to determine evaporation rates, an assumption is made, fixing the evaporation process at a constant speed. As a result the heat used for evaporation is constant throughout the tube. Also the last water droplets will only be evaporated just before they exit the heating tube. The gas flux ϕ_F in Nm3/h is the total bulk gas flow from the vortex tube. If the sampled portion of this value is multiplied with the density of water in the bulk gas in kg/m3 and corrected for conversion from m3 to Nm3 gives the amount of water in kg/s that passes through the tube.

$$X_{sample} = \frac{X * \phi_F}{3600} \frac{D_{sample}^2}{D_0^2} \tag{C.4}$$

X is the mass density of the nitrogen in the bulk gas; 0.025 kg/m3 of water is a reasonable upper limit in any real-case scenario.

The above explained model has been implemented in excel, allowing variation of all the specifications involving the heating tube and the gas flow characteristics.

Results Figure C.2 shows the result that is acquired when running the model with a specific setting. The characteristics of the heating tube are defined first; namely the diameter of the inner tube and power per meter of tube specified by the manufacturer. The flow speed, water content in the flow and inlet temperature can all be adjusted. Also an oulet temperature must be given. Using the given parameters, an estimation of required pipe length is returned in the form of the temperature graph.

The model has given a good approximation of heating capability of a heating tube at varying dimensions for the heating tube, sampling inlet system and pump system. Because all these components are linked and the combined sub-systems must match with each other this was no trivial task. Preventing over- or under dimensioning of

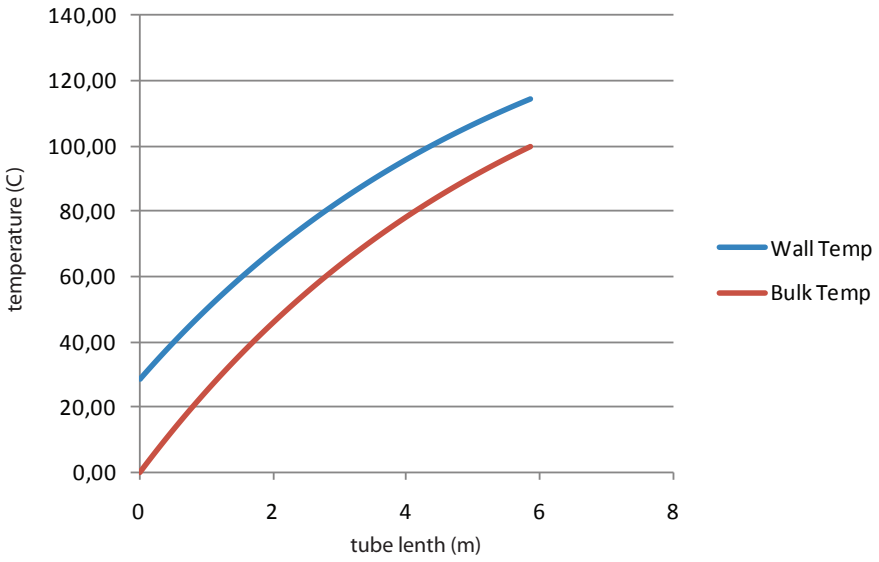

Figure C.2: The temperature curves of bulk gas flow and the tube inner wall as function of the tube position

certain parts of the system was avoided by modelling the heating tube performance beforehand.

Shortcomings of the model include the poor approximation of the evaporation-speed. In practice evaporation takes place as soon as possible, and this is likely to be more or less at the beginning of the tube. This also might play a role in the fact that the wall temperature at the heating tube inlet is much closer to the inlet gas temperature than the model predicts.

Appendix D

Matlab Script

Measurement Chamber SH calculation The matlab script used to calculate the specific humidity uses the pressure p, temperature T, and relative humidity RH of each probe as input. The uncertainties for these values are given by S_p, S_T and S_{RH}. Using equation 3.6, and converting to SH using equation 3.7.

The SH value is calculated for each combination of measurement values, thus for every second in the measurement. The uncertainty of the calculation is not evaluated because the effect of the partial vapour pressure in the equation is to complex. A rough calculation indicates that the theoretical error is actually very small.

Moist Gas Generation SH calculation For the determination of the SH of the moist gas that is produced, the water mass flux, or the slope of the weight graph $\phi_{m,w}$ is inserted manually. The mass flow of the Nitrogen carrier gas $\phi_{m,N}$ is obtained by converting the mass flow in normal cubic meters per hour $\phi_n omral$ ($S_{\phi_{normal}}$) using equation 6.1. The mixing ratio is obtained using equiation 6.1 and converted to the specific humidity using equation 3.7

Combining the above, the following equations are obtained for the generated ratio r_g and the specific humidity SH_g:

$$r_g = \frac{\phi_{n,w}/1000}{\frac{1.25}{3600}\phi_{normal}} \tag{D.1}$$

$$SH_g = \frac{r_g}{r_g+1} = \frac{2,88\phi_{n,w}}{\phi_{normal}\left(\frac{2.88\phi_{n,w}}{\phi_{normal}}+1\right)} \tag{D.2}$$

The uncertainty is calculated with 68% uncertainty intervals using:

$$S_{SH_r} = \sqrt{\left(\frac{\partial SH_g}{\partial \phi_{n,w}}\right)^2 \cdot S^2_{\phi_{n,w}} + \left(\frac{\partial SH_g}{\partial \phi_{normal}}\right)^2 \cdot S^2_{\phi_{normal}}} \tag{D.3}$$

Here $S_{\phi_{normal}}$ is the uncertainty of the mass flow meter, which is determined to be 0.02 m3n/h. $S_{\phi_{n,w}}$ is the uncertainty in the linear mass decrease in g/s. This value is returned by the fitting software used to determine the linear dependency of the mass curve.